AIMS Mathematics

https://www.aimspress.com/journal/Math

AIMS Mathematics, 11(9): 27585–27632.
DOI: 10.3934/math.20261104
Received: 19 June 2026
Revised: 17 August 2026
Accepted: 24 August 2026
Published: 01 September 2026

Research article

Augmenting push and pull search to improve threshold adaptive penalty function–based MOEA/D

Muhammad Sagheer[1], **Muhammad Asif Jan**[2,*], **Akhtar Munir Khan**[3], **Emel Khan**[1], **and Farman Shah**[3]

[1] Institute of Numerical Sciences, Kohat University of Science & Technology, Kohat 26000, Khyber Pakhtunkhwa, Pakistan

[2] College of Integrative Studies, Abdullah Al Salem University, Al Khaldiya 72303, Kuwait

[3] Department of Computing, Khanpur Institute of Technology, Rahim Yar Khan, Punjab 64100, Pakistan

* **Correspondence:** Email: muhammad.asif@aasu.edu.kw.

Abstract: CMOEA/D-TAP, which incorporates the threshold adaptive penalty (TAP) function into MOEA/D, has shown competitive performance on the CTP and CF benchmark suites. However, its effectiveness diminishes on more challenging CMOPs, such as DASCMOP, LIRCMOP, and MW, where a considerable number of function evaluations are consumed during the early optimization phase due to population stagnation and slow convergence toward the Pareto front. This behavior is primarily attributed to severe constraints, which prevent many solutions from reaching the constrained Pareto front (CPF) within the available evaluation budget. To overcome this limitation, CMOEA/D-TAP is enhanced by incorporating a push and pull search strategy, referred to as PPSTAP. The proposed algorithm operates in two distinct phases: a push phase that drives the population toward the unconstrained Pareto front, followed by a pull phase that guides solutions toward the CPF using an adaptive penalty function method. Extensive experiments on the CF, DASCMOP, LIRCMOP, and MW benchmark suites include sensitivity analysis against PPS and CMOEA/D-TAP and comparison of the best-performing variant, PPSTAP (p =20), with BiCo, C3M, and CCMO. Performance is evaluated using IGD, HV, and IGDp with statistical validation. The results show that all PPSTAP variants outperform their parent algorithms on average, while PPSTAP (p =20) achieves the best overall performance across constrained multiobjective optimization problems.

Keywords: constrained optimization; penalty function methods; push and pull search; evolutionary algorithm; multiobjective optimization based on decomposition
Mathematics Subject Classification: 68T20, 68W50, 90C59

1. Introduction

Optimization methods aim to identify the best possible solution(s) that optimize a given objective function while satisfying bound and/or functional constraints. The field has attracted significant research attention due to its wide range of real-world applications that rely on numerical modeling and decision-making. Optimization problems can be broadly classified into unconstrained and constrained formulations, continuous and combinatorial search spaces, and single-, multi-, or many-objective settings.

A large number of practical engineering and scientific problems can be modeled as constrained multiobjective optimization problems (CMOPs). Multiobjective evolutionary algorithms (MOEAs) have become a preferred choice for addressing such problems because of their robustness, flexibility, and ability to approximate the Pareto front efficiently. In many real-world scenarios, optimization tasks involve two or more conflicting objectives, naturally leading to multiobjective optimization problems (MOPs). These problems are often subject to various types of constraints, including bound, inequality, and equality constraints.

Without loss of generality, a constrained multiobjective optimization problem (CMOP) subject to functional and bound constraints can be formally expressed as follows [1, 2]:

$$\begin{aligned} \text{Minimize } & \mathbf{F}(\mathbf{x}) = (f_1(\mathbf{x}), f_2(\mathbf{x}), \ldots, f_M(\mathbf{x}))^T; \\ \text{Subject to } & c_k(\mathbf{x}) \geq 0,\ k = 1, 2, \ldots, q; \\ & x_i^{lb} \leq x_i \leq x_i^{ub},\ i = 1, 2 \ldots, n, \end{aligned} \tag{1.1}$$

where $\mathbf{x} = (x_1, \ldots, x_n)^T \in \mathcal{R}^n$ is the decision variables vector with n components, f_j, $j = 1, 2 \ldots, M$ are objectives, $\mathbf{F}$ is a vector of M objectives, and c_k's are q number of "greater equal to type" inequality constraints. f_j and c_k are functions of real variables which in nature, may be linear or non-linear. x_i^{lb} and x_i^{ub} are lower and upper bounds, respectively, to the i^{th} variable. These bounds constitute the search space, $\mathcal{S}$. A solution $\mathbf{x} \in \mathcal{S}$ that meets all imposed constraints in problem (1.1) is known as a feasible solution. While, if a solution violates any constraint of problem (1.1), it is called an infeasible solution. For a given solution $\mathbf{x} \in \mathcal{S}$, the overall violation of the constraints can be expressed as the sum of the individual violations [3]:

$$V(\mathbf{x}) = \sum_{k=1}^{q} \Big| \min(c_k(\mathbf{x}), 0) \Big|. \tag{1.2}$$

Moreover, $V(\mathbf{x}) = 0$ implies that $\mathbf{x}$ is feasible; otherwise, it is considered as infeasible.

In CMOPs, the objectives are often competing and inherently conflicting. For example, in the energy sector, two typical objectives are power output and fuel consumption. The former is generally required to be maximized, whereas the latter must be minimized. Similarly, for an economist of certain sector/industry, the objectives are to maximize profit/benefit and minimize loss [2]. In these examples, the objectives are in conflict with one another. Hence, the objectives frequently end up being at odds in multiobjective optimization. Therefore, it is difficult for a single solution to concurrently optimize all the objectives. In such cases, a group of compromised solutions are discovered.

The concept of *Pareto optimality* is widely employed to describe the most balanced trade-offs among conflicting objectives [1, 2]. Formally, a feasible solution vector $\mathbf{x}$ is said to be *Pareto-dominate* (i.e., "be better than") another feasible vector $\mathbf{y}$, denoted as $\mathbf{x} \preceq \mathbf{y}$, if $\mathbf{x}$ is at least as good as $\mathbf{y}$ in all objectives and strictly better in at least one objective. A feasible solution $\mathbf{x}^*$ is termed *Pareto optimal* for problem (1.1) if no other feasible vector $\mathbf{x}$ exists such that $\mathbf{F}(\mathbf{x}) \preceq \mathbf{F}(\mathbf{x}^*)$. The corresponding objective vector $\mathbf{F}(\mathbf{x}^*)$ is then called a *Pareto-optimal objective vector*. When neither $\mathbf{x}$ nor $\mathbf{y}$ dominates the other, both are referred to as *non-dominated solutions*. If a decision vector $\mathbf{x}$ is not dominated by any other feasible solution in the decision space, it is identified as a *Pareto-optimal decision vector*. The set of all such Pareto-optimal solutions constitutes the *Pareto Set* (*PS*), whereas the corresponding set of objective vectors in the objective space forms the *Pareto Front* (*PF*).

Practical optimization problems are constrained multiobjective in nature. For the solution of these problems, CMOEAs are employed. CMOEAs combine some constrained handling techniques with MOEAs, which are classified into various categories based on the CHTs [4]. Among these, Penalty function methods based CMOEAs are frequently used by the researchers in constrained multiobjective optimization as they push the solutions from both sides (feasible and infeasible) toward the optimal Pareto set. In challenging constrained optimization problems, it is difficult to keep solutions feasible from the start of the search until the end. Because the feasible region is often very narrow, solutions cannot move freely and are forced to follow limited paths. This causes many solutions to stay inactive or move very slowly in the early stages, while function evaluations continue to use up the provided budget. As a result, the solutions do not develop enough to reach the true Pareto front before the budget runs out. This shows a clear research gap: we need better methods that enable faster and more effective exploration of constrained search spaces.

The main contribution of this research is a mechanism that enables solutions to move more freely using a push initially and then obey constraints using a pull. The approach works in two phases. In the first phase, the algorithm pushes the population toward the unconstrained Pareto front, encouraging broad exploration. After a specified portion of the evaluation budget is used, the second phase begins, where a penalty-function method pulls the population back toward the feasible region to approximate the constrained Pareto front. This two-phase process helps balance exploration and constraint satisfaction more effectively.

The remainder of this paper is organized as follows. In Section 2, we provide a consolidated review of MOEA and CMOEA literature and a brief overview of alternative CMOP solution strategies, together with the motivation. In Section 3, we describe the proposed algorithmic framework. In Section 4, we illustrate system specifications, experimental setup, and performance evaluation metrics used in this study. In Section 5, we present the experimental results, comparisons, and rankings of the proposed scheme against four state-of-the-art algorithms. In Section 6, we discuss the simulation results of the competing algorithms. Finally, in Section 7, we conclude the paper with a summary of key findings and potential directions for future research.

2. Literature review

Many real world problems, like the robot gripper optimization problem [5], the combined economic emission dispatch (CEED) problem [6], the urban bus scheduling problem [7], and energy saving optimization problem [8] can be modeled as CMOPs. The applications of multiobjective optimization covers variety of problems from engineering sector to the field of industries. For instance mechanical design problem can be structured as CMOP, where a designer wants to optimize the design under some important restraints of resources and choices of decision makers [9]. Similarly, in the optimal power flow problem, minimization of fuel cost, emission, power losses, and voltage deviation can be modeled as CMOP [10].

2.1. Multiobjective optimization evolutionary algorithms (MOEAs)

Multiobjective Optimization Evolutionary Algorithms (MOEAs) are widely used to solve many optimization problems. They work well for real-world applications because they are fast and robust. They also relax strict requirements on objective functions and constraints, such as continuity or smoothness, which are often difficult to meet. MOEAs are extended versions of Evolutionary Algorithms (EAs). They use genetic operators, such as crossover and mutation, to generate new offspring from the parent population. A survival operator is then applied to select the best individuals for the next generation. Based on how they assign fitness values, MOEAs can be divided into three major categories, which are discussed in the following:

2.1.1. Pareto dominant based MOEAs

In this class of MOEAs, the fitness of each solution is assigned based on how many other solutions it dominates. A solution that dominates more solutions is considered more fit, while one that dominates fewer is considered less fit. These MOEAs also use different diversity-preservation techniques. The purpose is to obtain a well-spread set of solutions across the Pareto frontier. Some well-known algorithms in this class include NSGA [11], NSGA-II [12], NSGA-III [13], MOGA [14], NPGA [15], SPEA [16], SPEA-II [17], and PESA [18]. For more details, readers may refer to [19, 20]. This class of MOEAs maintains a good balance between convergence and diversity. However, their time complexity increases rapidly when the number of objectives becomes large. In other words, with many objectives, most solutions become non-dominated and share the same rank. As a result, the selection pressure becomes weak, and the algorithm fails to reach proper convergence.

2.1.2. Indicator based MOEAs

In indicator-based MOEAs, a quality indicator guides the evolutionary search. This indicator compares two or more approximations of the Pareto set. It assigns a numerical value to each approximation while keeping the dominance relation intact. Solutions that are closer to the Pareto-optimal front receive better indicator values, while those that lie farther from the front receive lower values. These indicator scores are then used during fitness evaluation. They enable the algorithm to decide which solutions should survive or move forward to the next generation. Common indicator-based MOEAs include IBEA [21], HypE [22], R2-IBEA [23], and IM-IBEA [24].

2.1.3. Decomposition based MOEAs

In decomposition-based MOEAs, each set of weight vectors converts the multiobjective problem into a single-objective one. This is done by taking a weighted sum of all objectives. In this way, the original vector optimization problem is split into several scalar subproblems. These subproblems run at the same time. This enables the algorithm to obtain many Pareto-optimal solutions in one simulation. In every subproblem, the objective function is an aggregated form of all objectives of the original MOP.

An example is given below for the subproblem formed using the Tchebycheff aggregation function:

$$\begin{aligned} \text{Minimize} \;\; & g^{tc}(\mathbf{x}|\mathbf{w}, \mathbf{z}^*) = \max_{1\le j\le M}\{w_j|f_j - z_j^*|\} \\ \text{Subject to} \;\; & c_k(\mathbf{x}) \ge 0,\, k = 1, 2, \ldots, q; \\ & x_i^{lb} \le x_i \le x_i^{ub},\, i = 1, 2 \ldots, n. \end{aligned} \tag{2.1}$$

In Eq (2.1), g^{tc} is the Tchybecheff aggregation function, $\mathbf{w} = (w_1, w_2, \ldots, w_M)$ is the weight vector and $\mathbf{z}^* = (z_1^*, z_2^*, \ldots, z_M^*)$ is approximation to the ideal/refrence point. Moreover,

$$z_j^* = \min\{f_j(\mathbf{x}) : \mathbf{x} \in \mathcal{S} : j = 1, 2, \ldots, M\} \tag{2.2}$$

Some other common aggregation functions used in this class of MOEAs are the weighted-sum method and the penalty boundary intersection (PBI) method. Several well-known algorithms also fall into this category. These include MOEA/D [3], MOEA/D-DE [25], MOEA/D-DRA [26], MOEA-DD [27], MOEA/D-AWA [28], MOEA/D-UR [29], MOEA/D-APP [30], MOEA/D-SCS [31], MOEA/D-WVA [32], MOEA/D-ADD [33], MOEA/D-HAE [34,35], MOEA/D-CSU [36].

2.2. Handling constraints in multiobjective optimization

Methods used to tackle the constraints in CMOPs are known as constraint-handling techniques (CHTs). Common CHTs include the penalty function method, the separation of objectives and constraints, the constraint domination principle (CDP) [37], and stochastic ranking (SR) [38]. Developments also include hybrid stochastic ranking (HSR) [39] and angle-based penalty functions [40]. For further details, readers may consult [41].

2.3. Penalty function methods

The penalty function method is a widely used and effective approach for constrained handling. It was first introduced in early works on single-objective optimization [42–44]. The core idea behind this technique is to transform a constrained problem into an unconstrained one. This is done by adding an extra term to the objective function. This term measures how much a solution violates the constraints. A scaling factor multiplies this violation term. Together, they form the penalty function. By optimizing this new penalty function, the algorithm guides the search toward feasible solutions. It reduces constraint violations while improving the objective value. In this way, the method provides a practical path to obtain constrained optimal solutions. Without loss of generality, the additive form of the penalty function can be expressed as:

$$g(\mathbf{x}) = f(\mathbf{x}) + \nu V(\mathbf{x}). \tag{2.3}$$

In this formulation, $g(\mathbf{x})$ is the extended penalty function. Parameter ν acts as the penalty weight. The term $V(\mathbf{x})$ shows the aggregate constraint violation for the decision vector $\mathbf{x}$. The product $\nu V(\mathbf{x})$ is known as the penalty term. Penalty functions are usually grouped into three types, based on how ν is handled. In static penalty methods, ν stays fixed during the entire optimization. In dynamic penalty methods, ν changes with the number of iterations. In adaptive penalty methods, ν is adjusted using feedback from the search process [37]. Penalty-based methods have an important advantage: They can be easily integrated into multiobjective evolutionary algorithms (MOEAs). This makes them effective for solving constrained multiobjective optimization problems (CMOPs) [45, 46]. By incorporating penalty terms into the objectives, solutions that violate constraints are discouraged, helping the algorithm focus on feasible regions.

2.4. *State-of-the-art CMOEAs*

Below, a brief review of several well-known state-of-the-art CMOEAs is given.

2.4.1. ANSGA-III

The Adaptive Non-dominated Sorting Genetic Algorithm (A-NSGA-III) [47] is an extended form of NSGA-III [13] developed for constrained optimization. NSGA-III is a refinement of NSGA-II [12]. It was originally introduced to address unconstrained Many-Objective Optimization Problems (MaOPs). In NSGA-III, the crowding distance used in NSGA-II is replaced with an adaptive reference-point mechanism. This change improves the diversity of solutions. A-NSGA-III builds on this framework to handle CMOPs and CMaOPs. It does so by using the Constraint Domination Principle (CDP) [48] as the constraint-handling technique and by applying a modified tournament selection.

2.4.2. BiCo

The Bi-directional Co-evolutionary CMOEA (BiCo) [49] is a new constraint-handling technique designed for CMOPs. It uses two co-evolving populations: A main population and an archive population. The main population pushes solutions toward the Pareto front (PF) from the feasible side. The archive population pushes solutions from the infeasible side. The main population is updated using NSGA-II and a modified form of CDP. The archive population is updated using an angle-based selection strategy [50].

2.4.3. CMOEAD

CMOEAD [51] is an extension of MOEA/D designed to solve CMOPs. In the original MOEA/D, parent–child selection is based on aggregation functions. CMOEAD modifies this step to handle constraints more effectively. In CMOEAD, two solutions are compared as follows: If both solutions have constraint violations that are below or equal to a given threshold, the comparison uses their aggregation function values. If this condition is not met, the comparison is based on their scaled constraint violations instead. The violation threshold is updated adaptively using the current feasible ratio.

2.4.4. CAEAD

The Constrained Alternative Evolution and Degeneration (CAEAD) algorithm [52] manages convergence, diversity, and feasibility at the same time. It uses a dual-population structure to avoid getting stuck in local optima. The algorithm works in two alternating stages. In the evolution stage, the secondary population moves toward the unconstrained Pareto front (PF). This step improves convergence and lowers the chance of local trapping. The main population focuses on maintaining feasibility. In the degeneration stage, both populations are pushed toward the constrained PF. This step enhances diversity and strengthens coverage of the feasible solution.

2.4.5. CCMO

The Co-evolutionary Constrained Multiobjective Optimizer (CCMO) [53] handles CMOPs by evolving two separate populations. The main population works on the original CMOP. The second population solves a simplified helper problem. This helper population guides the main population toward the Pareto front (PF) of the CMOP. In CCMO, the interaction between the two populations is weak compared to other multi-population methods. CCMO uses NSGA-II combined with CDP as its optimization engine.

2.4.6. CMOEA-MS

The Multi-Stage CMOEA, called CMOEA-MS [54], uses a staged evolutionary process to approximate the constrained Pareto front of CMOPs. It balances objective optimization with constraint satisfaction. The algorithm switches between two stages, called A and B. The switch depends on a predefined threshold parameter λ. When the feasible ratio of the combined population is lower than λ, the algorithm enters stage A. In this stage, objectives and constraint violations are treated with similar weight. When the feasible ratio is higher than λ, the algorithm moves to stage B. Here, feasibility is given more priority, while keeping the population diverse. Stage A pushes solutions toward the boundaries of the front. Stage B helps the solutions spread along the constrained PF.

2.4.7. ToP

The Two-Phase (ToP) framework [55] simultaneously addresses constraints in both decision and objective spaces of CMOPs. In the first phase, the CMOP is transformed into a constrained single-objective problem to identify promising feasible regions. In the second phase, a specific CMOEA is employed to refine the solutions and approximate the final PF.

2.4.8. C3M

The C3M algorithm [56] is a multi-stage method for solving CMOPs. In the first stage, it ignores feasibility and does not evaluate constraints. This helps the search explore the solution space more freely. In later stages, the algorithm introduces feasibility checks. By doing this, it gradually guides the search toward the constrained Pareto front (CPF). This multi-stage process enables the algorithm to reach the constrained PF faster.

2.4.9. PPS

PPS [57] applies the Push and Pull Search method within the MOEA/D framework. The approach works in two stages. In the first stage, the algorithm pushes the solutions toward the unconstrained Pareto front by ignoring all constraints. This step improves the convergence speed. In the second stage, the algorithm pulls the solutions toward the constrained Pareto front using CMOEA with ϵ constraints handling technique. These two stages together provide a good balance between convergence and diversity along the constrained Pareto front.

2.4.10. CMOEA/D-TAP

CMOEA/D-TAP [58] extends the Threshold Adaptive Penalty (TAP) framework to constrained multi-objective optimization by integrating adaptive penalty strategies into the decomposition-based MOEA/D algorithm. Five Near Feasibility Threshold (NFT) settings are introduced to adaptively penalize infeasible solutions based on their proximity to the feasible region, promoting an effective balance between constraint satisfaction and evolutionary search. The constraint-handling mechanism adopted by the best-performing CMOEA/D-TAP variant is presented below:

$$g_{tap}^{tc}(\mathbf{x}|\mathbf{w},\mathbf{z}^*) = g^{tc}(\mathbf{x}|\mathbf{w},\mathbf{z}^*) + (g_{feas}^{tc} - g_{all}^{tc})\left(\frac{V(\mathbf{x})}{\mu}\right); \tag{2.4}$$

where

$$\mu = \frac{0.07 \times V(\mathbf{x})}{V_{max}}, \quad V_{max} = \max\left\{V(\mathbf{x}) : \mathbf{x} \in \mathcal{S}_n(\mathbf{x})\right\}. \tag{2.5}$$

Equations (2.4) and (2.5) involve the following terms: (1) $g^{tc}(\mathbf{x}|\mathbf{w},\mathbf{z}^*)$, the Tchebycheff value of $\mathbf{x}$; (2) $V(\mathbf{x})$, the aggregate constraint violation; (3) g_{feas}^{tc}, the minimum Tchebycheff value among feasible solutions in the neighborhood $\mathcal{S}_n(\mathbf{x})$, or, if none exists, that of the neighboring solution with the smallest $V(\mathbf{x})$; (4) g_{all}^{tc}, the minimum Tchebycheff value among all neighboring solutions; (5) Vmax, the maximum aggregate constraint violation in $\mathcal{S}_n(\mathbf{x})$; (6) μ, the near-feasibility threshold (NFT), defined as 7% of the scaled normalized aggregate constraint violations within $\mathcal{S}_n(\mathbf{x})$; and (7) g_{tap}^{tc}, the penalized Tchebycheff value used for solution comparison. In CMOEA/D, each solution update is formulated as an independent subproblem, where every solution $\mathbf{x} \in Pop$ is associated with a neighborhood, $\mathcal{S}_n(\mathbf{x})$. Since $(g_{feas}^{tc} - g_{all}^{tc})$ and μ depend on the neighboring constraint violations, $V(\mathbf{x})$, they adapt throughout the search and differ across subproblems. Consequently, neighborhoods near the feasibility boundary receive smaller thresholds, whereas those farther away receive larger ones, rendering the resulting penalty inherently Threshold Adaptive. For numerical stability in MATLAB, μ is set to `realmin` when $V_{\max} = 0$, and any zero-valued $V(\mathbf{x})$ is similarly replaced with `realmin`.

2.5. Motivation

The CMOEAD-TAP [58] algorithm has demonstrated strong performance on classical benchmark suites such as CTP and CF. However, when applied to more intricate and highly constrained multiobjective optimization problems (CMOPs), a critical challenge emerges. During the initial phase of evolution, the population exhibits pronounced stagnation, with most candidate solutions either remaining static or advancing at an extremely slow rate. This sluggish progression consumes a substantial number of function evaluations. The root cause of this phenomenon lies in the presence of stringent and tightly coupled constraints that characterize these complex CMOPs. Such constraints effectively restrict the evolutionary search to exceedingly narrow feasible corridors. Navigating within these narrow regions inhibits exploratory movement, prevents smooth progression, and ultimately leads to premature stagnation of the search dynamics. A promising remedy is to relax the constraints temporarily in the early stage, enabling the population to be guided toward the unconstrained Pareto front. Once a predefined number of function evaluations has elapsed, the search can then be transitioned into a constraint-aware phase, during which solutions are gradually pulled toward the constrained Pareto front. This push and pull paradigm offers a structured mechanism to enhance exploratory capacity without compromising convergence to feasible optimal regions. Motivated by these observations, we aim to incorporate and refine such a push and pull strategy to significantly improve the search efficiency and robustness of evolutionary algorithms when tackling challenging and highly constrained CMOPs.

3. Proposed algorithmic framework

To overcome the premature stagnation of CMOEA/D-TAP [58] on highly constrained multi-objective optimization problems (CMOPs), we integrate a push–pull search strategy with the Threshold Adaptive Penalty (TAP) framework, yielding the proposed PPSTAP algorithm. The push phase performs unconstrained objective-driven exploration to avoid early stagnation, whereas the pull phase progressively activates the TAP mechanism (Eqs (2.4) and (2.5)) to guide the population toward the constrained Pareto front. This seamless transition from unconstrained exploration to adaptive constraint enforcement improves search diversity and convergence under complex constraints. The pseudo-code and flowchart of PPSTAP are presented in Algorithm 1 and Figure 1, respectively, followed by a detailed step-by-step illustration.

The algorithm begins by initializing the function evaluation counter, nFE, to zero (line 1). Next, N uniformly distributed m-dimensional weight vectors satisfying

$$\sum_{j=1}^{m} W_j^i = 1$$

are generated, and the T nearest weight vectors, determined using the Euclidean distance, define the neighborhood set $I(i)$ for each subproblem (line 2). Subsequently, N decision vectors are randomly initialized within the search space $\mathcal{S}$ (line 3) and evaluated to obtain their objective and constraint values, followed by the initialization of the reference vector $\mathbf{z}^*$ and the update of nFE (lines 4–5). The evolutionary process starts at line 6. For each solution $\mathbf{x}_i$ (line 7), the mating selection set $\mathcal{S}_n(\mathbf{x}_i)$ is selected from the neighborhood $I(i)$ with probability δ (lines 8–9) or from the entire population otherwise (line 11). Two distinct parents are then selected (line 12), differential evolution generates a trial vector (line 13), and polynomial mutation produces a bounded offspring (line 14), which is evaluated to update the reference vector $\mathbf{z}^*$ (lines 15–16). The Tchebycheff aggregation values and the corresponding NFT-based adaptive penalty values are subsequently computed for the offspring and its neighboring solutions (lines 17–18). Environmental selection follows a push–pull strategy. During the push phase, when $nFE < p\% \times MaxFE$ (line 19), constraint violations are ignored, and neighboring solutions are updated solely according to their Tchebycheff aggregation values, while the indices of improved solutions are stored in J_r (lines 20–22) to promote exploration. Once $nFE \geq p\% \times MaxFE$, the algorithm switches to the pull phase, where the NFT-based adaptive penalty mechanism guides the search toward the constrained Pareto front by jointly considering objective quality and constraint satisfaction (lines 27–29). Replacement is restricted to at most n_r neighboring solutions (lines 30–32), after which nFE is updated (line 33). Upon termination, the Pareto set (PS) and Pareto front (PF) are returned (line 34).

Algorithm 1: PPSTAP

Input: $maxFE,\ N,\ T,\ \delta,\ n_r$;

Output: Pareto Set (PS) and Pareto Front (PF);

Initialization $nFE \leftarrow 0$;

Generate weight vectors $W = \{\mathbf{w}^i\}_{i=1}^N$ and T nearest neighbors indices set $I(i)$;

Initialize $\{\mathbf{x}^i\}_{i=1}^N$ uniformly and evaluate each to get $\mathbf{F}(\mathbf{x}^i)$ and $V(\mathbf{x}^i)$;

$\mathbf{z}^* \leftarrow \min_i \mathbf{F}(\mathbf{x}^i)$;

$nFE \leftarrow nFE + N$;

while $nFE < maxFE$ **do**

    for $i \leftarrow 1$ **to** N **do**

        if $rand < \delta$ **then**

            $\mathcal{S}_n(\mathbf{x_i}) \leftarrow I(i)/I(i)$ are neighboring indices for x_i ;

        else

            $\mathcal{S}_n(\mathbf{x_i}) \leftarrow \{1, \ldots, N\}$;

        Randomly pick distinct $i_1, i_2 \in \mathcal{S}_n(\mathbf{x_i})$;

        Create trial $\mathbf{v}^{i'}$ via DE from $\mathbf{x}^i, \mathbf{x}^{i_1}, \mathbf{x}^{i_2}$ with F (scaling) = 0.5 and P_{CR} (crossover probability) = 0.95 ;

        After polynomial mutation $\mathbf{v}^i \leftarrow \mathbf{v}^{i'}$, with $P_{PM} = \frac{1}{n}$ and clip $\mathbf{v}^i$ to bounds;

        Evaluate $\mathbf{F}(\mathbf{v}^i)$ and $V(\mathbf{v}^i)$;

        $\mathbf{z}^* \leftarrow \min(\mathbf{z}^*, \mathbf{F}(\mathbf{v}^i))$;

        Compute $g^{tc}(\mathbf{v}^i|\mathbf{w}^{\mathcal{S}_n(\mathbf{x_i})}, \mathbf{z}^*)$ and $g^{tc}(\mathbf{x}^i|\mathbf{w}^i, \mathbf{z}^*)$;

        Compute $g^{tc}_{tap}(\mathbf{v}^i|\mathbf{w}^{\mathcal{S}_n(\mathbf{x_i})}, \mathbf{z}^*)$ and $g^{tc}_{tap}(\mathbf{x}^i|\mathbf{w}^i, \mathbf{z}^*)$;

        if $nFE < p\,\% \times maxFE$ **then**

            if $any\,(g^{tc}(\mathbf{v}^i|\mathbf{w}^l, \mathbf{z}^*) < g^{tc}(\mathbf{x}^l|\mathbf{w}^l, \mathbf{z}^*))\,for\ l \in \mathcal{S}_n(\mathbf{x_i})$ **then**

                $Indices \leftarrow \{l \in \mathcal{S}_n(\mathbf{x_i}) \mid g^{tc}(\mathbf{v}^i|\mathbf{w}^l, \mathbf{z}^*) < g^{tc}(\mathbf{x}^l|\mathbf{w}^l, \mathbf{z}^*)\}$;

                $J_r \leftarrow \mathcal{S}_n(\mathbf{x_i})(Indices)$;

                if $|J_r| > n_r$ **then**

                    $J_r \leftarrow \text{randsample}(J_r, n_r)$;

                Replace $\mathbf{x}^{J_r} \leftarrow \mathbf{v}^i$, $\mathbf{F}(\mathbf{x}^{J_r}) \leftarrow \mathbf{F}(\mathbf{v}^i)$, and $\mathbf{V}(\mathbf{x}^{J_r}) \leftarrow \mathbf{V}(\mathbf{v}^i)$;

        else

            if $any\,(g^{tc}_{tap}(\mathbf{v}^i|\mathbf{w}^l, \mathbf{z}^*) < g^{tc}_{tap}(\mathbf{x}^l|\mathbf{w}^l, \mathbf{z}^*))\,for\ l \in \mathcal{S}_n(\mathbf{x_i})$ **then**

                $Indices \leftarrow \{l \in \mathcal{S}_n(\mathbf{x_i}) \mid g^{tc}_{tap}(\mathbf{v}^i|\mathbf{w}^l, \mathbf{z}^*) < g^{tc}_{tap}(\mathbf{x}^l|\mathbf{w}^l, \mathbf{z}^*)\}$;

                $J_r \leftarrow \mathcal{S}_n(\mathbf{x_i})(Indices)$;

                if $|J_r| > n_r$ **then**

                    $J_r \leftarrow \text{randsample}(J_r, n_r)$;

                Replace $\mathbf{x}^{J_r} \leftarrow \mathbf{v}^i$, $\mathbf{F}(\mathbf{x}^{J_r}) \leftarrow \mathbf{F}(\mathbf{v}^i)$, and $\mathbf{V}(\mathbf{x}^{J_r}) \leftarrow \mathbf{V}(\mathbf{v}^i)$;

    $nFE \leftarrow nFE + N$;

return $PS\ and\ PF$;

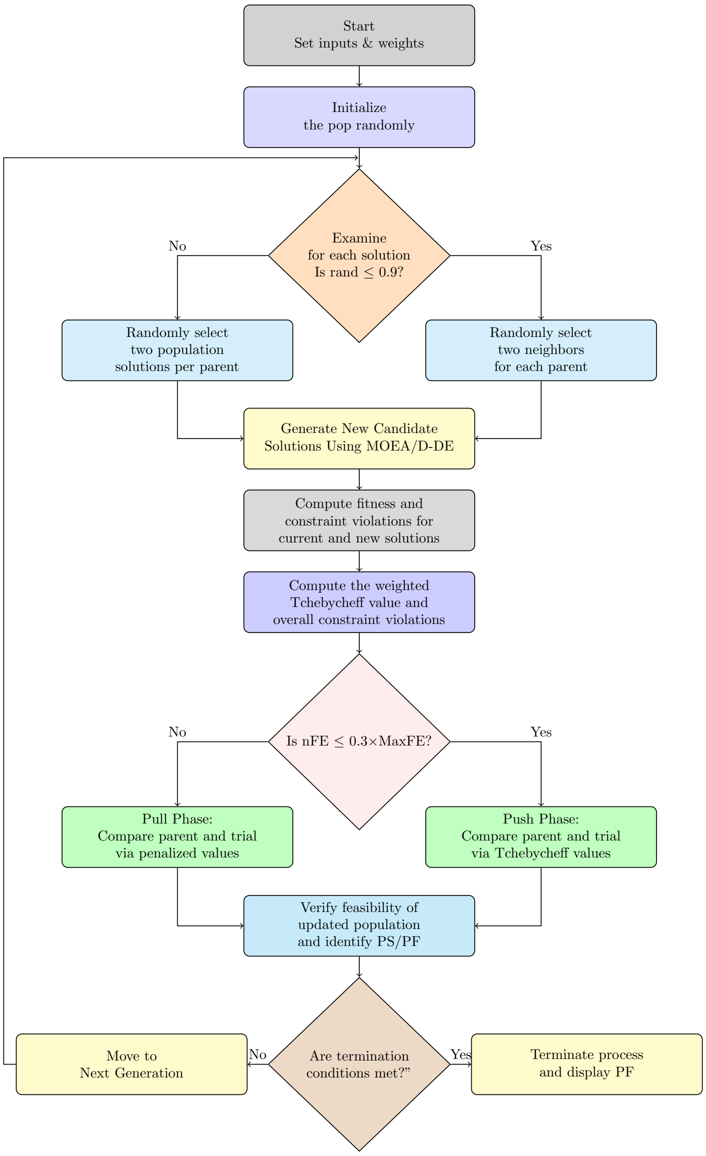

Figure 1. Flow chart of the proposed algorithm.

3.1. Distinctive features of PPSTAP

PPSTAP integrates the complementary strengths of PPS and CMOEA/D-TAP. Unlike PPS, which employs the ϵ-constraint handling technique and switches from the push phase to the pull phase based on the distance between the ideal and nadir points, PPSTAP adopts the TAP function for constraint handling and transitions between the two phases after consuming $p\%$ of the available function evaluations. In contrast to CMOEA/D-TAP, PPSTAP incorporates the push–pull search strategy to improve the balance between exploration and exploitation. Consequently, PPSTAP combines the search mechanism of PPS with the adaptive constraint-handling capability of CMOEA/D-TAP within a unified optimization framework.

4. Experimental set up

To validate the performance of the proposed algorithm against the state-of-the-art competitors, the following experimental setup is adopted.

4.1. Computer system specifications and used flatform

The experiments were conducted on a system running Windows 11 Pro. The machine used an AMD Ryzen 5 5600U processor at 2.30 GHz and had 16 GB of RAM. All coding and computational work was carried out using MATLAB R2023a. To ensure a fair testing environment for all algorithms, the simulations were performed through the PlatEMO platform [59]. PlatEMO includes MATLAB implementations of the benchmark algorithms used in this study. The implementation of the proposed method was added to the same platform for consistency. General experimental settings, such as population size, maximum function evaluations, and the number of independent runs, were kept the same for every algorithm. However, each algorithm's internal parameters were left at their default values, as stated in their original papers and provided within PlatEMO.

4.2. Benchmark test functions

In evolutionary optimization, especially in multiobjective problems, new algorithms are usually evaluated on a set of benchmark test functions. For unconstrained multiobjective tasks, the quality of an algorithm is mainly judged by its convergence and diversity along the Pareto front. However, when constraints are introduced, the algorithm must also identify and explore feasible regions. This makes the search process more challenging. In this study, the proposed method was evaluated through sensitivity and comparative analyses. The evaluation was carried out on four benchmark suites, each offering different types of difficulties for constrained multiobjective search. The benchmarks used in this work included CF [60], LIRCMOP [61], DASCMOP [62], and MW [63] series, which are detailed below.

4.2.1. CF series

The CF benchmark suite comprises ten CMOPs, including seven bi-objective (CF1–CF7) and three tri-objective (CF8–CF10) problems with diverse constrained Pareto front (CPF) characteristics. CF1 features a discrete CPF; CF2 and CF3 contain disconnected convex and non-convex branches, respectively; CF4–CF7 exhibit continuous CPFs with mixed convex and non-convex regions; and CF8–CF10 comprise multiple disconnected three-dimensional Pareto surfaces. The CPFs of CF1–CF3 and CF8–CF10 form subsets of the unconstrained Pareto front (UPF), whereas those of CF4–CF7 largely coincide with the UPF. However, the suite does not include constraints that induce discontinuities in the decision space

4.2.2. DASCMOPs series

DASCMOPs include nine constrained multiobjective problems that are adjustable and scalable. This benchmark suite is constructed to evaluate CMOPs against three principal challenges: diversity maintenance, feasibility preservation, and convergence efficiency. The difficulty level is controlled through three parameters: η, ξ, and γ. In this study, we used the default values of these parameters provided in PlatEMO. DASCMOP1 to DASCMOP6 have two objective functions. DASCMOP7 to DASCMOP9 compose of three objective functions.

4.2.3. LIRCMOPs series

The LIRCMOP test suite contains fourteen benchmark problems. In these CMOPs, the search space is largely infeasible, with feasible regions being comparatively limited. Because of this imbalance, CMOEAs often struggle to locate high-quality constrained optimal solutions. In addition, the suite includes several challenging characteristics. These include convex and non-convex constraint Pareto fronts (CPFs), disconnected CPFs, and search spaces with major discontinuities. Such features can easily trap algorithms around local CPFs and slow their progress. Furthermore, LIRCMOP1 to LIRCMOP12 are two objective problems, while LIRCMOP13 and LIRCMOP14 are three objective problems.

4.2.4. MW series

The MW suite provides fourteen CMOPs with varying difficulty. MW4, MW8, and MW14 support three scalable objectives, while the others include two objectives. The suite covers several challenge types, including nonlinear constraints, nonlinear CPF structures, scalability in variables and objectives, discontinuous feasible regions, and disconnected objective spaces.

4.3. Performance evaluation metrics

To assess the performance of the algorithms in terms of convergence and diversity, we used three metrics. These metrics evaluated how effectively the algorithms converged. They also measured the diversity of the solutions. A detailed explanation of these metrics is provided below.

4.3.1. Inverted generational distance (IGD) metric

The Inverted Generational Distance (IGD) is a widely used performance indicator for evaluating the convergence and diversity of MOEAs/CMOEAs. Let P^* denote a representative set of points on the true Pareto front (PF) and $\mathcal{A}$ the approximation set obtained by an algorithm. IGD is defined as the average distance from P^* to $\mathcal{A}$ as follows [64, 65]:

$$\begin{aligned} IGD(P^*, \mathcal{A}) &= \frac{\sum_{y^* \in P^*} d(y^*, \mathcal{A})}{|P^*|}, \\ (y^*, \mathcal{A}) &= \min_{y \in \mathcal{A}} \left(\sqrt{\sum_{j=1}^{j=m} (y_j^* - y_j)^2} \right). \end{aligned} \tag{4.1}$$

The Euclidean distance $d(y^*, \mathcal{A})$ measures the proximity of $y^* \in P^*$ to $\mathcal{A}$. IGD averages these distances over P^*, with lower values indicating better convergence and diversity, provided that P^* is well distributed.

4.3.2. Hyper-Volume (HV) metric

The HV metric represents the closeness of an approximation to the true PF [66, 67]. That is, the HV calculated the region dominated by the true PF approximated set and a reference point in the objective space. More specifically, let $\mathcal{A}$ be an approximation to the true PF, and $\mathbf{z}^r = [z_1^r, z_2^r, \ldots, z_m^r]^T$ be the reference point in objective space. Thus,

$$HV(\mathcal{A}) = VOL\left(\bigcup_{\mathbf{x}\in A}[f_1(\mathbf{x}), z_1^r] \times \ldots [f_m(\mathbf{x}), z_m^r]\right), \tag{4.2}$$

where $VOL(.)$ is the Lebesgue measure representing the measure of the region dominated by the approximating set $\mathcal{A}$. Further, for two different approximation sets, the one with larger HV value better approximates the true PF.

4.3.3. Inverted generational distance plus (IGDp) metric

The IGD metric may not satisfy Pareto compliance. In other words, for two different approximations, $\mathcal{A}$ and $\mathcal{B}$, it is possible that IGD($\mathcal{A}$) ≤ IGD($\mathcal{B}$), while $\mathcal{B}$ actually Pareto dominates $\mathcal{A}$ (see [68, 69] for details). Now, let $\mathcal{A}$ be an approximation of the Pareto set for the true Pareto front (PF), and let P^* be the set of representative solutions from the true PF. The IGDp metric is defined as follows:

$$\begin{aligned} IGDp(P^*, \mathcal{A}) &= \frac{\sum_{y^*\in P^*} \tilde{d}(y^*, \mathcal{A})}{|P^*|}, \\ \tilde{d}(y^*, \mathcal{A}) &= \min_{y\in\mathcal{A}}\left(\sqrt{\sum_{j=1}^{j=m}(\max\{y_j^* - y_j, 0\})^2}\right). \end{aligned} \tag{4.3}$$

4.4. Parameter settings

The proposed algorithm involves sensitive and fixed parameters. The experimental settings adopted throughout this study are described below.

4.4.1. Sensitivity analysis of parameter p

The influence of control parameter p is assessed using four values, namely p = 10, 20, 30, and 40. Each value defines a distinct variant of the proposed algorithm, enabling a systematic evaluation of parameter sensitivity.

4.4.2. Fixed parameter settings

To ensure a fair comparison with the competing algorithms, all experiments were performed using the following parameter settings:

- Population size: $N = 100$ for all CMOPs;
- Neighborhood size: $T = 10$;
- DE scaling factor: $F = 0.5$;

- DE crossover probability: $P_{\mathrm{CR}} = 0.95$;
- Polynomial mutation probability: $P_{\mathrm{PM}} = \frac{1}{D}$;
- Maximum number of replaced solutions: $n_r = 1$;
- Neighborhood selection probability: $\delta = 0.9$;
- Maximum number of function evaluations: $MaxFE = 300{,}000$ for all problems and algorithms;
- Number of independent runs: 30 for each algorithm on every test problem.

5. Simulation results

In this section, the results of the sensitivity and comparative analyses are presented.

5.1. Sensitivity analysis

The PPSTAP variants obtained through the sensitivity analysis of parameter p were evaluated against their parent algorithms, PPS and CMOEA/D-TAP. Tables 1–3 report the mean (SD) values of the IGD, HV, and IGDp metrics for the competing algorithms, with the best results highlighted. Statistical significance was evaluated using the Wilcoxon Rank-Sum and Friedman tests [70] based on the IGD, HV, and IGDp indicators and results are presented in the Tables 4–7. Figures 2–4 illustrate the mean IGD, HV, and IGDp convergence over the first six problems of each benchmark suite. Figures 5–8 depict the Pareto fronts from the best run (minimum IGD) for representative CF (2, 4, 5, 6), DASCMOP (1, 2, 4, 5), LIRCMOP (5, 10, 12, 13), and MW (2, 5, 6, 13) problems.

5.2. Comparative analysis

The best-performing variant, PPSTAP (p =20), was further compared with the state-of-the-art algorithms BiCo, C3M, and CCMO. Tables 8–10 display the mean (SD) values of metrics, IGD, HV, and IGDp, for the compared algorithms, with the best values highlighted. Statistical comparisons were performed using the Wilcoxon Rank-Sum and Friedman tests [70] based on the IGD, HV, and IGDp indicators, with the results summarized in Tables 11 and 12. Figures 9–4 present the mean IGD, HV, and IGDp convergence profiles for the first six problems of each benchmark suite. Figures 5–8 depict the Pareto fronts of the best run (lowest IGD) for representative problems from the CF (2, 4, 5, 6, 8, 9), DASCMOP (1, 2, 4, 5, 6, 7), LIRCMOP (1, 2, 5, 10, 12, 13), and MW (2, 5, 6, 8, 9, 13) suites.

5.3. Explanation of Statistical Results

The Wilcoxon rank-sum and Friedman test results are presented for each benchmark suite, with the overall summary reported in the final column. In the tables, the notation a/b/c indicates the number of benchmark problems on which a competing algorithm performs statistically better than, worse than, or equivalently to the reference algorithm over 30 independent runs. Owing to the limitations of the PlatEMO platform, the Friedman test was conducted on a reduced benchmark set comprising CF1–CF9 (9 problems), DASCMOP1–DASCMOP4 and DASCMOP9 (5 problems), LIRCMOP1–LIRCMOP14 (14 problems), and MW3–MW7, MW9, and MW11–MW14 (10 problems).

Table 1. Mean and standard deviation of IGD values for comparative analysis.

Problem	M	D	PPS	CMOEA/D-TAP	PPSTAP (p =10)	PPSTAP (p =30)	PPSTAP (p =40)	PPSTAP (p =20)
CF1	2	10	1.1353e-3 (3.85e-4)	1.8987e-3 (6.23e-4)	2.0060e-3 (6.51e-4)	2.7717e-3 (8.89e-4)	3.4111e-3 (8.69e-4)	2.2580e-3 (4.84e-4)
CF2	2	10	3.8657e-3 (8.46e-4)	5.9290e-3 (8.63e-4)	5.8323e-3 (1.19e-3)	5.7999e-3 (1.12e-3)	6.2470e-3 (8.64e-4)	5.2311e-3 (4.82e-4)
CF3	2	10	2.4936e-1 (1.54e-1)	1.6957e-1 (7.81e-2)	1.6966e-1 (7.80e-2)	2.2103e-1 (6.17e-2)	1.8222e-1 (9.18e-2)	2.1044e-1 (1.18e-1)
CF4	2	10	4.6472e-2 (3.97e-2)	1.8036e-2 (1.65e-2)	1.2768e-2 (4.46e-3)	1.1518e-2 (2.26e-3)	1.3184e-2 (2.79e-3)	1.2080e-2 (2.25e-3)
CF5	2	10	2.3741e-1 (7.69e-2)	2.3376e-1 (1.19e-1)	2.2272e-1 (1.08e-1)	2.1670e-1 (1.07e-1)	2.1203e-1 (1.03e-1)	1.3855e-1 (7.92e-2)
CF6	2	10	3.8432e-2 (1.26e-2)	4.2743e-2 (8.97e-3)	3.0071e-2 (1.40e-2)	2.4218e-2 (1.24e-2)	2.5699e-2 (1.35e-2)	2.3311e-2 (1.15e-2)
CF7	2	10	2.2165e-1 (7.54e-2)	1.9771e-1 (1.04e-1)	1.5676e-1 (7.58e-2)	1.6428e-1 (8.95e-2)	1.5844e-1 (8.90e-2)	1.6582e-1 (9.30e-2)
CF8	3	10	1.7986e-1 (1.59e-2)	1.2950e-1 (7.75e-3)	1.3023e-1 (5.78e-3)	1.3416e-1 (7.70e-3)	1.3357e-1 (5.90e-3)	1.3062e-1 (8.28e-3)
CF9	3	10	1.1028e-1 (1.70e-2)	8.5235e-2 (3.76e-3)	8.5135e-2 (3.53e-3)	8.5337e-2 (2.83e-3)	8.3885e-2 (3.52e-3)	8.4495e-2 (3.08e-3)
CF10	3	10	2.5178e-1 (6.19e-2)	2.7450e-1 (1.57e-1)	1.8154e-1 (4.24e-2)	1.9450e-1 (4.64e-2)	1.8512e-1 (4.72e-2)	1.7664e-1 (4.01e-2)
DASCMOP1	2	30	1.9689e-1 (2.40e-1)	1.2336e-1 (2.25e-1)	7.0651e-3 (1.06e-3)	8.2117e-3 (1.85e-3)	8.9947e-3 (2.42e-3)	7.5893e-3 (7.39e-4)
DASCMOP2	2	30	5.1397e-3 (1.50e-4)	2.1840e-2 (3.13e-2)	6.9005e-3 (7.01e-4)	7.9147e-3 (8.89e-4)	8.5084e-3 (1.44e-3)	7.7942e-3 (1.35e-3)
DASCMOP3	2	30	2.7975e-1 (1.09e-1)	3.3665e-1 (2.41e-2)	1.3349e-1 (9.47e-2)	7.4314e-2 (5.03e-2)	8.0661e-2 (5.95e-2)	4.5343e-2 (1.98e-2)
DASCMOP4	2	30	1.4162e-1 (7.93e-2)	6.9277e-2 (8.77e-2)	8.7286e-2 (9.09e-2)	3.3546e-2 (6.78e-2)	3.9462e-2 (7.27e-2)	2.7497e-2 (6.17e-2)
DASCMOP5	2	30	4.1814e-3 (2.78e-4)	4.4246e-3 (3.97e-4)	4.3840e-3 (1.56e-4)	4.4243e-3 (2.89e-4)	4.5088e-3 (3.67e-4)	4.3719e-3 (1.80e-4)
DASCMOP6	2	30	1.4266e-1 (2.40e-1)	1.2639e-1 (1.62e-1)	1.0145e-1 (1.36e-1)	4.0033e-2 (9.15e-2)	3.4457e-2 (2.97e-2)	2.0588e-2 (2.28e-3)
DASCMOP7	3	30	5.6347e-2 (6.46e-3)	8.5167e-2 (6.07e-2)	6.7292e-2 (3.30e-2)	7.4284e-2 (5.87e-2)	7.6843e-2 (5.77e-2)	1.0421e-1 (7.11e-2)
DASCMOP8	3	30	6.9237e-2 (7.72e-3)	7.6736e-2 (1.77e-2)	7.7187e-2 (1.20e-2)	9.8061e-2 (5.32e-2)	1.5435e-1 (1.28e-1)	9.8559e-2 (4.95e-2)
DASCMOP9	3	30	1.3870e-1 (1.17e-1)	2.8731e-1 (1.29e-1)	1.6716e-1 (7.76e-2)	1.3475e-1 (4.76e-3)	1.3500e-1 (6.61e-3)	1.3239e-1 (5.98e-3)
LIRCMOP1	2	30	8.0991e-3 (2.75e-3)	5.7377e-2 (2.80e-2)	1.8909e-2 (9.70e-3)	2.7713e-2 (1.16e-2)	2.3296e-2 (9.94e-3)	2.2850e-2 (1.32e-2)
LIRCMOP2	2	30	6.3190e-3 (8.77e-4)	7.3117e-2 (2.26e-2)	2.1577e-2 (7.87e-3)	2.0848e-2 (8.05e-3)	2.6954e-2 (1.12e-2)	2.1454e-2 (8.65e-3)
LIRCMOP3	2	30	5.8335e-3 (2.92e-3)	1.8281e-1 (4.37e-2)	6.7965e-2 (2.73e-2)	7.6538e-2 (4.35e-2)	7.6962e-2 (3.79e-2)	5.1342e-2 (1.51e-2)
LIRCMOP4	2	30	4.3657e-2 (6.18e-2)	1.9668e-1 (3.52e-2)	4.9273e-2 (1.54e-2)	5.1937e-2 (2.27e-2)	4.9616e-2 (1.89e-2)	5.3675e-2 (2.14e-2)
LIRCMOP5	2	30	6.8228e-3 (8.34e-4)	1.1473e+0 (2.16e-1)	4.5974e-3 (2.90e-4)	4.4871e-3 (1.27e-4)	4.4743e-3 (1.79e-4)	4.4899e-3 (1.59e-4)
LIRCMOP6	2	30	5.2086e-2 (2.44e-1)	1.3456e+0 (4.99e-4)	4.2740e-3 (2.12e-4)	4.2014e-3 (1.49e-4)	4.1539e-3 (1.29e-4)	4.1978e-3 (1.68e-4)
LIRCMOP7	2	30	1.0770e-1 (4.12e-2)	1.6256e+0 (3.03e-1)	2.4600e-2 (2.92e-2)	1.0315e+0 (2.48e+0)	2.3574e+0 (7.70e+0)	8.5001e-3 (2.42e-3)
LIRCMOP8	2	30	1.0733e-1 (5.45e-2)	1.5722e+0 (4.16e-1)	2.1291e-2 (2.69e-2)	7.3422e-3 (4.32e-4)	7.6556e-3 (5.99e-4)	7.8578e-3 (9.06e-4)
LIRCMOP9	2	30	3.5741e-1 (1.09e-1)	7.1400e-1 (1.12e-1)	3.2923e-1 (1.55e-1)	6.4589e-3 (3.15e-4)	6.3670e-3 (1.62e-4)	2.6500e-2 (3.83e-2)
LIRCMOP10	2	30	3.0417e-2 (6.46e-2)	3.5350e-1 (8.68e-2)	7.2012e-3 (1.47e-4)	7.0709e-3 (1.35e-4)	7.0436e-3 (1.49e-4)	7.1309e-3 (1.74e-4)
LIRCMOP11	2	30	2.5556e-1 (6.30e-2)	4.2047e-1 (8.37e-2)	8.2109e-2 (6.62e-2)	2.1046e-1 (1.55e-1)	1.2220e-1 (7.45e-2)	1.7413e-1 (1.11e-1)
LIRCMOP12	2	30	1.3389e-1 (5.18e-2)	3.7894e-1 (1.65e-1)	9.8976e-2 (1.38e-1)	3.3510e-2 (4.76e-2)	1.0897e-1 (1.16e-1)	7.4638e-3 (3.93e-3)
LIRCMOP13	3	30	1.2733e-1 (3.36e-3)	1.3131e+0 (7.71e-4)	1.3784e-1 (2.31e-3)	1.3567e-1 (1.42e-3)	1.3462e-1 (1.99e-3)	1.3546e-1 (1.19e-3)
LIRCMOP14	3	30	1.1838e-1 (3.50e-3)	1.2348e+0 (1.90e-1)	1.3815e-1 (1.54e-3)	1.4777e-1 (9.23e-3)	1.5808e-1 (1.94e-2)	1.4093e-1 (4.10e-3)
MW1	2	15	2.7107e-3 (9.97e-5)	3.2185e-3 (1.99e-5)	3.2118e-3 (2.07e-5)	3.1922e-3 (2.59e-5)	3.1908e-3 (2.55e-5)	3.1980e-3 (2.54e-5)
MW2	2	15	1.8030e-1 (9.89e-2)	4.2419e-3 (1.46e-4)	3.9138e-3 (9.33e-5)	4.4040e-3 (2.16e-4)	4.0011e-3 (2.03e-5)	3.9859e-3 (3.15e-5)
MW3	2	15	6.5573e-3 (8.84e-4)	4.2117e-3 (1.10e-4)	4.2636e-3 (1.40e-4)	4.3948e-3 (1.99e-4)	4.3139e-3 (2.25e-4)	4.1948e-3 (1.02e-4)
MW4	3	15	5.4646e-2 (1.96e-3)	6.1635e-2 (7.29e-4)	6.1531e-2 (5.77e-4)	6.1573e-2 (6.48e-4)	6.2152e-2 (1.23e-3)	6.1642e-2 (6.55e-4)
MW5	2	15	3.7654e-1 (3.72e-1)	7.7891e-3 (1.93e-3)	5.3178e-3 (2.23e-3)	8.9155e-3 (1.99e-3)	8.3448e-3 (3.02e-3)	5.8625e-3 (2.06e-3)
MW6	2	15	6.3100e-1 (3.65e-1)	3.9769e-3 (7.37e-5)	3.9518e-3 (2.39e-5)	3.9598e-3 (3.67e-5)	3.9661e-3 (5.90e-5)	3.9500e-3 (8.32e-6)
MW7	2	15	5.6229e-3 (5.27e-4)	4.7154e-3 (7.82e-5)	4.6694e-3 (8.40e-5)	4.7624e-3 (1.09e-4)	4.7169e-3 (8.07e-5)	4.6776e-3 (8.20e-5)
MW8	3	15	1.4123e-1 (5.34e-2)	7.0181e-2 (2.12e-3)	6.8612e-2 (1.59e-3)	7.1489e-2 (2.24e-3)	7.0303e-2 (2.29e-3)	6.8520e-2 (1.26e-3)
MW9	2	15	4.3822e-2 (1.36e-1)	6.8859e-3 (1.21e-3)	5.8184e-3 (7.36e-4)	5.1605e-3 (9.62e-4)	4.8748e-3 (2.52e-4)	4.8093e-3 (4.56e-4)
MW10	2	15	3.8271e-1 (2.31e-1)	4.4192e-3 (2.05e-5)	4.4309e-3 (3.67e-5)	4.4512e-3 (4.21e-5)	4.4418e-3 (3.46e-5)	4.4420e-3 (4.93e-5)
MW11	2	15	7.4724e-3 (4.15e-4)	1.0081e-2 (6.96e-5)	1.1537e-2 (1.07e-3)	1.1798e-2 (2.44e-3)	1.1830e-2 (1.46e-3)	1.1324e-2 (9.06e-4)
MW12	2	15	2.9853e-2 (1.21e-1)	4.9381e-3 (5.91e-5)	4.9055e-3 (5.99e-5)	5.0440e-3 (8.43e-5)	5.0102e-3 (1.09e-4)	4.9377e-3 (3.98e-5)
MW13	2	15	4.9892e-1 (4.16e-1)	1.9589e-2 (6.61e-4)	2.2761e-2 (1.39e-3)	2.5606e-2 (5.55e-3)	2.3639e-2 (6.41e-3)	2.3025e-2 (3.74e-3)
MW14	3	15	1.3694e-1 (2.20e-2)	3.7818e-1 (4.06e-2)	3.9200e-1 (3.10e-2)	3.6342e-1 (3.59e-2)	3.7768e-1 (3.89e-2)	3.6034e-1 (3.08e-2)

Table 2. Mean and standard deviation of HV values for comparative analysis.

Problem	M	D	PPS	CMOEA/D-TAP	PPSTAP (p =10)	PPSTAP (p =30)	PPSTAP (p =40)	PPSTAP (p =20)
CF1	2	10	5.6473e-1 (4.70e-4)	5.6338e-1 (8.78e-4)	5.6322e-1 (9.40e-4)	5.6218e-1 (1.26e-3)	5.6134e-1 (1.21e-3)	5.6291e-1 (6.82e-4)
CF2	2	10	6.7653e-1 (2.25e-3)	6.7351e-1 (2.09e-3)	6.7345e-1 (2.10e-3)	6.7360e-1 (1.82e-3)	6.7302e-1 (1.28e-3)	6.7419e-1 (1.55e-3)
CF3	2	10	1.9214e-1 (5.42e-2)	2.3134e-1 (4.11e-2)	2.2258e-1 (4.30e-2)	2.0345e-1 (3.48e-2)	2.3052e-1 (4.05e-2)	2.1117e-1 (5.12e-2)
CF4	2	10	4.8523e-1 (3.89e-2)	5.1236e-1 (2.02e-2)	5.1947e-1 (4.89e-3)	5.2121e-1 (2.72e-3)	5.1946e-1 (3.06e-3)	5.1957e-1 (3.92e-3)
CF5	2	10	3.3375e-1 (4.34e-2)	3.5329e-1 (7.39e-2)	3.6769e-1 (6.88e-2)	3.6514e-1 (7.03e-2)	3.6824e-1 (6.45e-2)	4.2144e-1 (4.54e-2)
CF6	2	10	6.5688e-1 (1.30e-2)	6.5335e-1 (8.03e-3)	6.6684e-1 (1.32e-2)	6.7219e-1 (1.31e-2)	6.7044e-1 (1.39e-2)	6.7229e-1 (1.17e-2)
CF7	2	10	4.5080e-1 (8.79e-2)	5.3141e-1 (6.43e-2)	5.3369e-1 (6.55e-2)	5.2288e-1 (8.41e-2)	5.1666e-1 (9.23e-2)	5.1416e-1 (9.45e-2)
CF8	3	10	3.4141e-1 (1.52e-2)	3.9745e-1 (1.26e-2)	3.9803e-1 (8.95e-3)	3.9200e-1 (1.34e-2)	3.9102e-1 (9.86e-3)	3.9787e-1 (1.08e-2)
CF9	3	10	4.3151e-1 (2.45e-2)	4.4788e-1 (1.20e-2)	4.4891e-1 (9.53e-3)	4.4961e-1 (7.76e-3)	4.5246e-1 (7.94e-3)	4.5286e-1 (8.26e-3)
CF10	3	10	2.2828e-1 (3.87e-2)	2.4284e-1 (7.50e-2)	2.7975e-1 (3.40e-2)	2.7532e-1 (2.98e-2)	2.7594e-1 (3.35e-2)	2.8381e-1 (4.31e-2)
DASCMOP1	2	30	1.6792e-1 (5.15e-2)	1.8330e-1 (4.74e-2)	2.1051e-1 (1.16e-3)	2.1004e-1 (1.51e-3)	2.0940e-1 (1.82e-3)	2.1053e-1 (1.23e-3)
DASCMOP2	2	30	3.5483e-1 (9.12e-5)	3.4500e-1 (1.40e-2)	3.5377e-1 (1.13e-3)	3.5288e-1 (1.42e-3)	3.5209e-1 (2.08e-3)	3.5291e-1 (1.87e-3)
DASCMOP3	2	30	2.2621e-1 (3.40e-2)	2.1310e-1 (1.37e-2)	2.7814e-1 (1.85e-2)	2.8761e-1 (1.05e-2)	2.8512e-1 (1.21e-2)	2.9330e-1 (7.20e-3)
DASCMOP4	2	30	1.7366e-1 (1.71e-2)	1.8898e-1 (2.01e-2)	1.8546e-1 (2.01e-2)	1.9729e-1 (1.50e-2)	1.9602e-1 (1.62e-2)	1.9868e-1 (1.38e-2)
DASCMOP5	2	30	3.5112e-1 (1.80e-4)	3.5108e-1 (3.42e-4)	3.5116e-1 (1.46e-4)	3.5115e-1 (2.04e-4)	3.5113e-1 (1.74e-4)	3.5118e-1 (1.16e-4)
DASCMOP6	2	30	2.5775e-1 (1.06e-1)	2.6587e-1 (7.32e-2)	2.7637e-1 (6.73e-2)	3.0276e-1 (4.73e-2)	3.0795e-1 (9.61e-3)	3.1232e-1 (2.58e-4)
DASCMOP7	3	30	2.7975e-1 (2.60e-3)	2.6239e-1 (3.32e-2)	2.7246e-1 (1.96e-2)	2.7021e-1 (3.07e-2)	2.6758e-1 (3.21e-2)	2.5066e-1 (3.89e-2)
DASCMOP8	3	30	2.0039e-1 (1.26e-3)	1.9360e-1 (1.45e-2)	1.9370e-1 (1.04e-2)	1.7991e-1 (3.66e-2)	1.5056e-1 (6.62e-2)	1.7691e-1 (3.49e-2)
DASCMOP9	3	30	1.8101e-1 (2.73e-2)	1.4720e-1 (2.70e-2)	1.7453e-1 (1.87e-2)	1.8257e-1 (2.80e-3)	1.8294e-1 (3.29e-3)	1.8307e-1 (2.32e-3)
LIRCMOP1	2	30	2.3661e-1 (8.26e-4)	2.0400e-1 (1.58e-2)	2.3124e-1 (4.33e-3)	2.2572e-1 (5.99e-3)	2.2756e-1 (4.76e-3)	2.2841e-1 (6.74e-3)
LIRCMOP2	2	30	3.5956e-1 (3.79e-4)	3.1821e-1 (1.18e-2)	3.5025e-1 (3.82e-3)	3.4931e-1 (6.42e-3)	3.4628e-1 (7.55e-3)	3.4918e-1 (6.36e-3)
LIRCMOP3	2	30	2.0530e-1 (1.52e-3)	1.3575e-1 (1.38e-2)	1.7976e-1 (1.20e-2)	1.7700e-1 (1.52e-2)	1.7545e-1 (1.44e-2)	1.8558e-1 (7.34e-3)
LIRCMOP4	2	30	2.9833e-1 (2.85e-2)	2.3006e-1 (1.42e-2)	2.9396e-1 (7.40e-3)	2.9317e-1 (1.06e-2)	2.9370e-1 (8.82e-3)	2.9240e-1 (1.06e-2)
LIRCMOP5	2	30	2.9161e-1 (3.15e-4)	9.5724e-3 (5.24e-2)	2.9117e-1 (3.82e-4)	2.9129e-1 (2.66e-4)	2.9134e-1 (3.51e-4)	2.9132e-1 (3.69e-4)
LIRCMOP6	2	30	1.9049e-1 (3.60e-2)	0.0000e+0 (0.00e+0)	1.9683e-1 (2.95e-4)	1.9685e-1 (2.36e-4)	1.9694e-1 (3.19e-4)	1.9687e-1 (2.44e-4)
LIRCMOP7	2	30	2.5245e-1 (1.59e-2)	9.5430e-3 (5.23e-2)	2.8424e-1 (1.21e-2)	2.1814e-1 (1.27e-1)	1.8133e-1 (1.35e-1)	2.9161e-1 (1.98e-3)
LIRCMOP8	2	30	2.5491e-1 (1.76e-2)	1.8359e-2 (7.00e-2)	2.8604e-1 (1.16e-2)	2.9289e-1 (4.74e-4)	2.9263e-1 (7.54e-4)	2.9225e-1 (9.81e-4)
LIRCMOP9	2	30	4.5265e-1 (4.77e-2)	2.4301e-1 (6.84e-2)	4.4084e-1 (6.32e-2)	5.6579e-1 (6.14e-4)	5.6594e-1 (5.41e-4)	5.6016e-1 (1.10e-2)
LIRCMOP10	2	30	6.9609e-1 (2.98e-2)	5.2340e-1 (5.04e-2)	7.0580e-1 (4.68e-4)	7.0618e-1 (4.37e-4)	7.0614e-1 (5.08e-4)	7.0603e-1 (4.79e-4)
LIRCMOP11	2	30	5.3434e-1 (4.11e-2)	4.9029e-1 (2.19e-2)	6.8383e-1 (3.18e-2)	6.0243e-1 (8.48e-2)	6.6076e-1 (4.52e-2)	6.2669e-1 (4.61e-2)
LIRCMOP12	2	30	5.6134e-1 (2.35e-2)	4.4141e-1 (8.23e-2)	5.8159e-1 (7.33e-2)	6.1134e-1 (1.41e-2)	5.7553e-1 (6.05e-2)	6.1962e-1 (1.95e-3)
LIRCMOP13	3	30	5.2051e-1 (3.95e-3)	3.4275e-4 (7.01e-5)	4.7939e-1 (7.67e-3)	4.8704e-1 (4.44e-3)	4.8978e-1 (8.93e-3)	4.8629e-1 (4.82e-3)
LIRCMOP14	3	30	5.3248e-1 (3.66e-3)	1.3018e-2 (6.66e-2)	4.9351e-1 (7.70e-3)	4.8983e-1 (9.92e-3)	4.8612e-1 (1.65e-2)	4.9361e-1 (5.52e-3)
MW1	2	15	4.8880e-1 (1.53e-4)	4.8842e-1 (3.11e-4)	4.8860e-1 (2.93e-4)	4.8878e-1 (3.58e-4)	4.8892e-1 (3.40e-4)	4.8880e-1 (3.82e-4)
MW2	2	15	3.5939e-1 (1.02e-1)	5.8155e-1 (3.26e-4)	5.8219e-1 (1.37e-4)	5.8161e-1 (2.80e-4)	5.8210e-1 (2.37e-5)	5.8212e-1 (3.69e-5)
MW3	2	15	5.4333e-1 (1.22e-3)	5.4559e-1 (2.90e-4)	5.4592e-1 (1.48e-4)	5.4576e-1 (1.81e-4)	5.4596e-1 (9.23e-5)	5.4596e-1 (1.07e-4)
MW4	3	15	8.1965e-1 (4.06e-3)	7.8015e-1 (3.45e-3)	7.8387e-1 (5.27e-3)	7.7807e-1 (3.71e-3)	7.7907e-1 (4.18e-3)	7.8169e-1 (3.58e-3)
MW5	2	15	2.0455e-1 (1.16e-1)	3.1982e-1 (1.02e-3)	3.2168e-1 (9.89e-4)	3.1946e-1 (1.02e-3)	3.1983e-1 (1.46e-3)	3.2145e-1 (1.02e-3)
MW6	2	15	8.7510e-2 (8.13e-2)	3.2771e-1 (5.26e-5)	3.2777e-1 (2.11e-5)	3.2774e-1 (3.47e-5)	3.2775e-1 (3.69e-5)	3.2778e-1 (1.35e-5)
MW7	2	15	4.1226e-1 (2.15e-4)	4.1204e-1 (1.54e-4)	4.1228e-1 (1.54e-4)	4.1214e-1 (1.50e-4)	4.1220e-1 (1.62e-4)	4.1225e-1 (1.33e-4)
MW8	3	15	3.3744e-1 (9.25e-2)	4.7896e-1 (1.18e-2)	4.8929e-1 (8.56e-3)	4.7152e-1 (9.71e-3)	4.7716e-1 (1.20e-2)	4.9080e-1 (8.08e-3)
MW9	2	15	3.6558e-1 (7.77e-2)	3.9054e-1 (3.21e-3)	3.9379e-1 (2.09e-3)	3.9610e-1 (2.72e-3)	3.9715e-1 (1.31e-3)	3.9757e-1 (1.87e-3)
MW10	2	15	2.3345e-1 (1.08e-1)	4.5427e-1 (5.08e-5)	4.5431e-1 (1.33e-4)	4.5406e-1 (3.16e-4)	4.5430e-1 (1.41e-4)	4.5422e-1 (2.57e-4)
MW11	2	15	4.4756e-1 (1.28e-4)	4.4710e-1 (7.17e-5)	4.4547e-1 (1.70e-3)	4.4468e-1 (2.81e-3)	4.4469e-1 (2.17e-3)	4.4561e-1 (1.26e-3)
MW12	2	15	5.8153e-1 (1.06e-1)	6.0458e-1 (1.40e-4)	6.0478e-1 (9.08e-5)	6.0423e-1 (3.40e-4)	6.0440e-1 (2.52e-4)	6.0465e-1 (1.05e-4)
MW13	2	15	2.5956e-1 (1.30e-1)	4.7470e-1 (3.96e-4)	4.7340e-1 (8.45e-4)	4.7278e-1 (1.68e-3)	4.7371e-1 (1.97e-3)	4.7356e-1 (1.34e-3)
MW14	3	15	4.5461e-1 (4.27e-3)	3.9603e-1 (1.14e-2)	3.9020e-1 (9.41e-3)	3.9616e-1 (1.29e-2)	3.9200e-1 (9.62e-3)	3.9764e-1 (8.39e-3)

Table 3. Mean and standard deviation of IGDp values for comparative analysis.

Problem	M	D	PPS	CMOEA/D-TAP	PPSTAP (p =10)	PPSTAP (p =30)	PPSTAP (p =40)	PPSTAP (p =20)
CF1	2	10	1.1353e-3 (3.85e-4)	1.8987e-3 (6.23e-4)	2.0060e-3 (6.51e-4)	2.7717e-3 (8.89e-4)	3.4111e-3 (8.69e-4)	2.2580e-3 (4.84e-4)
CF2	2	10	3.1493e-3 (6.15e-4)	5.0082e-3 (7.02e-4)	4.8916e-3 (1.04e-3)	4.8607e-3 (8.77e-4)	5.1243e-3 (7.13e-4)	4.4395e-3 (4.63e-4)
CF3	2	10	2.3402e-1 (1.46e-1)	1.5439e-1 (6.64e-2)	1.6028e-1 (7.06e-2)	2.0692e-1 (5.19e-2)	1.6704e-1 (7.98e-2)	1.9605e-1 (1.09e-1)
CF4	2	10	3.9327e-2 (3.10e-2)	1.7237e-2 (1.60e-2)	1.1752e-2 (3.33e-3)	1.0459e-2 (1.67e-3)	1.1638e-2 (2.08e-3)	1.1236e-2 (2.05e-3)
CF5	2	10	1.7784e-1 (4.98e-2)	1.6743e-1 (7.90e-2)	1.5275e-1 (7.28e-2)	1.5427e-1 (7.57e-2)	1.5125e-1 (6.91e-2)	9.5598e-2 (4.83e-2)
CF6	2	10	3.4042e-2 (1.14e-2)	3.7573e-2 (7.45e-3)	2.4978e-2 (1.20e-2)	2.0210e-2 (1.20e-2)	2.2025e-2 (1.22e-2)	1.9997e-2 (1.05e-2)
CF7	2	10	1.6832e-1 (6.45e-2)	1.2875e-1 (7.04e-2)	1.0629e-1 (4.40e-2)	1.1499e-1 (6.25e-2)	1.2052e-1 (6.45e-2)	1.2143e-1 (7.07e-2)
CF8	3	10	1.2610e-1 (9.12e-3)	9.6643e-2 (7.09e-3)	9.3781e-2 (4.98e-3)	9.7963e-2 (6.56e-3)	9.8705e-2 (5.26e-3)	9.5200e-2 (5.61e-3)
CF9	3	10	7.6292e-2 (1.43e-2)	6.1289e-2 (2.53e-3)	6.0732e-2 (2.99e-3)	6.1022e-2 (2.42e-3)	6.0102e-2 (2.94e-3)	6.0356e-2 (2.24e-3)
CF10	3	10	2.1805e-1 (6.86e-2)	2.5277e-1 (1.55e-1)	1.5850e-1 (4.68e-2)	1.7483e-1 (5.19e-2)	1.6395e-1 (5.03e-2)	1.5165e-1 (4.27e-2)
DASCMOP1	2	30	1.5901e-1 (1.74e-1)	9.6016e-2 (1.61e-1)	4.6101e-3 (1.19e-3)	5.4132e-3 (2.07e-3)	6.1560e-3 (2.71e-3)	4.7031e-3 (9.28e-4)
DASCMOP2	2	30	3.9589e-3 (1.38e-4)	1.2448e-2 (1.87e-2)	4.5576e-3 (1.91e-4)	5.2009e-3 (2.58e-4)	5.4712e-3 (4.54e-4)	5.0578e-3 (4.67e-4)
DASCMOP3	2	30	1.5849e-1 (6.00e-2)	1.8343e-1 (2.07e-2)	6.1890e-2 (4.52e-2)	3.6648e-2 (2.55e-2)	4.1993e-2 (2.99e-2)	2.2106e-2 (1.22e-2)
DASCMOP4	2	30	1.3971e-1 (7.79e-2)	6.8039e-2 (8.81e-2)	8.6168e-2 (9.14e-2)	3.2097e-2 (6.81e-2)	3.8037e-2 (7.31e-2)	2.6050e-2 (6.21e-2)
DASCMOP5	2	30	3.0512e-3 (3.02e-4)	2.8679e-3 (4.89e-4)	2.7928e-3 (2.40e-4)	2.8625e-3 (3.47e-4)	2.8895e-3 (3.76e-4)	2.7602e-3 (1.94e-4)
DASCMOP6	2	30	1.2719e-1 (2.45e-1)	9.7110e-2 (1.60e-1)	7.5956e-2 (1.32e-1)	2.5503e-2 (9.35e-2)	1.4470e-2 (1.66e-2)	6.2696e-3 (3.70e-4)
DASCMOP7	3	30	4.6328e-2 (5.27e-3)	7.5927e-2 (6.50e-2)	5.6295e-2 (3.63e-2)	6.2835e-2 (6.18e-2)	6.6326e-2 (6.17e-2)	9.7183e-2 (7.54e-2)
DASCMOP8	3	30	2.9455e-2 (1.80e-3)	3.9511e-2 (2.18e-2)	3.9638e-2 (1.53e-2)	6.2417e-2 (6.15e-2)	1.2596e-1 (1.42e-1)	6.6599e-2 (5.86e-2)
DASCMOP9	3	30	8.0863e-2 (8.51e-2)	1.8471e-1 (8.91e-2)	8.8906e-2 (6.38e-2)	5.4422e-2 (3.35e-3)	5.3846e-2 (4.25e-3)	5.4139e-2 (3.33e-3)
LIRCMOP1	2	30	6.1131e-3 (1.44e-3)	5.1684e-2 (2.50e-2)	1.2580e-2 (5.53e-3)	1.9328e-2 (7.89e-3)	1.6409e-2 (6.76e-3)	1.6058e-2 (9.48e-3)
LIRCMOP2	2	30	5.5981e-3 (6.42e-4)	4.0225e-2 (1.27e-2)	1.4296e-2 (4.24e-3)	1.3967e-2 (4.38e-3)	1.7850e-2 (6.34e-3)	1.4316e-2 (4.77e-3)
LIRCMOP3	2	30	4.8199e-3 (2.29e-3)	1.5813e-1 (3.50e-2)	4.5027e-2 (1.76e-2)	4.8130e-2 (2.24e-2)	5.1560e-2 (2.31e-2)	3.6673e-2 (1.19e-2)
LIRCMOP4	2	30	2.6252e-2 (3.80e-2)	1.2057e-1 (2.35e-2)	3.0222e-2 (8.93e-3)	3.2104e-2 (1.38e-2)	3.0790e-2 (1.09e-2)	3.3722e-2 (1.26e-2)
LIRCMOP5	2	30	5.1150e-3 (5.79e-4)	1.1440e+0 (2.16e-1)	3.5724e-3 (3.31e-4)	3.4301e-3 (1.58e-4)	3.4569e-3 (1.98e-4)	3.4394e-3 (1.75e-4)
LIRCMOP6	2	30	4.9294e-2 (2.45e-1)	1.3456e+0 (4.99e-4)	3.3311e-3 (2.58e-4)	3.2165e-3 (1.88e-4)	3.1564e-3 (1.81e-4)	3.2174e-3 (2.23e-4)
LIRCMOP7	2	30	9.1777e-2 (3.37e-2)	1.6255e+0 (3.04e-1)	2.1180e-2 (2.56e-2)	9.6123e-1 (2.45e+0)	2.2614e+0 (7.71e+0)	6.6502e-3 (2.33e-3)
LIRCMOP8	2	30	9.3564e-2 (4.81e-2)	1.5719e+0 (4.17e-1)	1.8498e-2 (2.43e-2)	5.4913e-3 (4.09e-4)	5.7768e-3 (6.02e-4)	6.0139e-3 (9.04e-4)
LIRCMOP9	2	30	1.9085e-1 (7.12e-2)	5.7564e-1 (1.26e-1)	2.5084e-1 (1.30e-1)	4.6228e-3 (2.70e-4)	4.4986e-3 (2.05e-4)	1.7484e-2 (2.64e-2)
LIRCMOP10	2	30	2.3316e-2 (4.86e-2)	2.6960e-1 (6.42e-2)	5.0195e-3 (1.55e-4)	4.8243e-3 (1.17e-4)	4.7936e-3 (1.41e-4)	4.9548e-3 (1.74e-4)
LIRCMOP11	2	30	1.9826e-1 (4.84e-2)	3.0752e-1 (7.60e-2)	1.9601e-2 (3.91e-2)	1.3507e-1 (1.26e-1)	4.8649e-2 (5.78e-2)	9.9285e-2 (5.98e-2)
LIRCMOP12	2	30	9.6986e-2 (3.87e-2)	2.9735e-1 (1.65e-1)	8.1816e-2 (1.21e-1)	2.6941e-2 (4.09e-2)	8.6136e-2 (9.08e-2)	4.8038e-3 (4.00e-3)
LIRCMOP13	3	30	6.8758e-2 (2.83e-3)	1.3120e+0 (7.30e-4)	9.8203e-2 (7.19e-3)	9.1513e-2 (2.77e-3)	8.9007e-2 (5.66e-3)	9.1500e-2 (2.57e-3)
LIRCMOP14	3	30	5.9915e-2 (2.54e-3)	1.2332e+0 (1.92e-1)	8.8599e-2 (4.52e-3)	9.3156e-2 (1.05e-2)	1.0140e-1 (2.23e-2)	8.8766e-2 (3.44e-3)
MW1	2	15	2.2438e-3 (9.28e-5)	2.3774e-3 (4.27e-5)	2.3119e-3 (2.40e-5)	2.3361e-3 (3.95e-5)	2.2777e-3 (2.32e-5)	2.2918e-3 (2.93e-5)
MW2	2	15	1.8020e-1 (9.88e-2)	3.0034e-3 (1.06e-4)	2.7675e-3 (6.60e-5)	3.1145e-3 (1.53e-4)	2.8293e-3 (1.43e-5)	2.8184e-3 (2.23e-5)
MW3	2	15	3.5632e-3 (7.11e-4)	2.0646e-3 (6.09e-5)	1.9775e-3 (5.67e-5)	2.0403e-3 (6.17e-5)	1.9732e-3 (4.83e-5)	1.9604e-3 (5.14e-5)
MW4	3	15	3.9672e-2 (1.51e-3)	4.4859e-2 (7.52e-4)	4.3975e-2 (4.24e-4)	4.5654e-2 (7.60e-4)	4.5140e-2 (1.01e-3)	4.4158e-2 (5.28e-4)
MW5	2	15	1.7115e-1 (1.63e-1)	7.3490e-3 (1.63e-3)	4.9917e-3 (1.75e-3)	8.1678e-3 (1.60e-3)	7.4987e-3 (2.09e-3)	5.5174e-3 (1.72e-3)
MW6	2	15	5.9797e-1 (3.33e-1)	1.8667e-3 (8.72e-5)	1.8265e-3 (3.12e-5)	1.8461e-3 (5.01e-5)	1.8478e-3 (7.19e-5)	1.8262e-3 (1.52e-5)
MW7	2	15	2.4080e-3 (1.51e-4)	2.2315e-3 (8.20e-5)	2.1066e-3 (6.45e-5)	2.2045e-3 (6.34e-5)	2.1639e-3 (6.42e-5)	2.1268e-3 (6.03e-5)
MW8	3	15	1.3627e-1 (5.60e-2)	5.2427e-2 (5.20e-3)	4.7966e-2 (3.75e-3)	5.5219e-2 (4.21e-3)	5.2827e-2 (4.63e-3)	4.7605e-2 (3.34e-3)
MW9	2	15	3.9885e-2 (1.26e-1)	5.3727e-3 (1.15e-3)	4.2531e-3 (6.98e-4)	3.7039e-3 (9.51e-4)	3.3800e-3 (2.37e-4)	3.2981e-3 (4.43e-4)
MW10	2	15	3.3182e-1 (1.86e-1)	2.5520e-3 (1.38e-5)	2.5386e-3 (9.32e-6)	2.5631e-3 (1.86e-5)	2.5423e-3 (1.47e-5)	2.5463e-3 (1.73e-5)
MW11	2	15	3.6269e-3 (2.26e-4)	4.0478e-3 (1.18e-4)	4.4756e-3 (4.21e-4)	4.6511e-3 (6.62e-4)	4.6158e-3 (4.40e-4)	4.4143e-3 (3.53e-4)
MW12	2	15	2.6569e-2 (1.17e-1)	2.8958e-3 (6.41e-5)	2.7963e-3 (5.33e-5)	3.0476e-3 (8.55e-5)	2.9898e-3 (8.33e-5)	2.8680e-3 (6.44e-5)
MW13	2	15	4.8682e-1 (4.23e-1)	6.9081e-3 (1.59e-4)	7.1818e-3 (4.02e-4)	7.9793e-3 (1.38e-3)	7.5467e-3 (1.19e-3)	7.3300e-3 (6.78e-4)
MW14	3	15	7.8509e-2 (1.16e-2)	1.9179e-1 (1.66e-2)	1.9059e-1 (9.09e-3)	1.8554e-1 (1.21e-2)	1.8770e-1 (1.54e-2)	1.8427e-1 (1.25e-2)

Table 4. Wilcoxon test results based on IGD values for sensitivity analysis.

Reference	Competitor	CF	DASCMOP	LIRCMOP	MW	Overall
PPSTAP (p =10)	PPS	2/7/1	4/1/4	6/7/1	4/10/0	16/25/6
	CMOEA/D-TAP	0/2/8	0/4/5	0/14/0	2/7/5	2/27/18
	PPSTAP (p =20)	3/0/7	3/3/3	6/2/6	3/2/9	15/7/25
	PPSTAP (p =30)	1/3/6	0/2/7	5/4/5	3/7/4	9/16/22
	PPSTAP (p =40)	0/2/8	0/3/6	6/4/4	2/6/6	8/15/24
PPSTAP (p =20)	PPS	2/7/1	4/3/2	6/8/0	4/10/0	16/28/3
	CMOEA/D-TAP	1/4/5	0/5/4	0/14/0	2/7/5	3/30/14
	PPSTAP (p =10)	0/3/7	3/3/3	2/6/6	2/3/9	7/15/25
	PPSTAP (p =30)	0/2/8	1/3/5	2/4/8	0/7/7	3/16/28
	PPSTAP (p =40)	0/3/7	0/5/4	2/4/8	0/7/7	2/19/26
PPSTAP (p =30)	PPS	2/6/2	3/2/4	7/7/0	4/10/0	16/25/6
	CMOEA/D-TAP	3/2/5	0/5/4	0/14/0	8/2/4	11/23/13
	PPSTAP (p =10)	3/1/6	2/0/7	4/5/5	7/3/4	16/9/22
	PPSTAP (p =20)	2/0/8	3/1/5	4/2/8	7/0/7	16/3/28
	PPSTAP (p =40)	1/3/6	1/3/5	3/4/7	2/1/11	7/11/29
PPSTAP (p =40)	PPS	2/6/2	3/3/3	6/6/2	4/10/0	15/25/7
	CMOEA/D-TAP	2/2/6	1/4/4	1/13/0	5/3/6	9/22/16
	PPSTAP (p =10)	2/0/8	3/0/6	4/6/4	6/2/6	15/8/24
	PPSTAP (p =20)	3/0/7	5/0/4	4/2/8	7/0/7	19/2/26
	PPSTAP (p =30)	3/1/6	3/1/5	4/3/7	1/2/11	11/7/29

Table 5. Wilcoxon test results based on HV values for sensitivity analysis.

Reference	Competitor	CF	DASCMOP	LIRCMOP	MW	Overall
PPSTAP (p =10)	PPS	2/8/0	3/2/4	7/6/1	4/9/1	16/25/6
	CMOEA/D-TAP	0/1/9	0/4/5	0/14/0	3/11/0	3/30/14
	PPSTAP (p =20)	1/0/9	3/2/4	6/1/7	2/2/10	12/5/30
	PPSTAP (p =30)	1/2/7	2/1/6	5/4/5	1/10/3	9/17/21
	PPSTAP (p =40)	0/2/8	0/3/6	4/4/6	2/7/5	6/16/25
PPSTAP (p =20)	PPS	2/7/1	3/4/2	7/7/0	3/9/2	15/27/5
	CMOEA/D-TAP	1/2/7	0/5/4	0/14/0	2/10/2	3/31/13
	PPSTAP (p =10)	0/1/9	2/3/4	1/6/7	2/2/10	5/12/30
	PPSTAP (p =30)	1/3/6	1/1/7	2/3/9	0/11/3	4/18/25
	PPSTAP (p =40)	0/4/6	1/4/4	2/3/9	0/6/8	3/17/27
PPSTAP (p =30)	PPS	2/7/1	2/3/4	8/6/0	4/9/1	16/25/6
	CMOEA/D-TAP	2/2/6	0/5/4	0/14/0	5/5/4	7/26/14
	PPSTAP (p =10)	2/1/7	1/2/6	4/5/5	10/1/3	17/9/21
	PPSTAP (p =20)	3/1/6	1/1/7	3/2/9	11/0/3	18/4/25
	PPSTAP (p =40)	1/2/7	0/0/9	1/1/12	7/0/7	9/3/35
PPSTAP (p =40)	PPS	2/8/0	2/3/4	7/5/2	3/9/2	14/25/8
	CMOEA/D-TAP	2/1/7	1/4/4	0/14/0	2/7/5	5/26/16
	PPSTAP (p =10)	2/0/8	3/0/6	4/4/6	7/2/5	16/6/25
	PPSTAP (p =20)	4/0/6	4/1/4	3/2/9	6/0/8	17/3/27
	PPSTAP (p =30)	2/1/7	0/0/9	1/1/12	0/7/7	3/9/35

Table 6. Wilcoxon test results based on IGDp values for sensitivity analysis.

Reference	Competitor	CF	DASCMOP	LIRCMOP	MW	Overall
PPSTAP (p =10)	PPS	2/6/2	3/2/4	7/6/1	4/10/0	16/24/7
	CMOEA/D-TAP	0/2/8	0/4/5	0/14/0	2/11/1	2/31/14
	PPSTAP (p =20)	1/0/9	3/2/4	6/1/7	3/2/9	13/5/29
	PPSTAP (p =30)	1/3/6	1/2/6	5/4/5	1/11/2	8/20/19
	PPSTAP (p =40)	0/2/8	0/3/6	5/4/5	2/6/6	7/15/25
PPSTAP (p =20)	PPS	2/7/1	3/4/2	6/8/0	4/10/0	15/29/3
	CMOEA/D-TAP	1/4/5	0/5/4	0/14/0	2/10/2	3/33/11
	PPSTAP (p =10)	0/1/9	2/3/4	1/6/7	2/3/9	5/13/29
	PPSTAP (p =30)	0/2/8	1/2/6	3/2/9	0/12/2	4/18/25
	PPSTAP (p =40)	0/4/6	1/4/4	3/5/6	0/6/8	4/19/24
PPSTAP (p =30)	PPS	2/6/2	2/3/4	7/7/0	4/10/0	15/26/6
	CMOEA/D-TAP	2/1/7	0/4/5	0/14/0	7/3/4	9/22/16
	PPSTAP (p =10)	3/1/6	2/1/6	4/5/5	11/1/2	20/8/19
	PPSTAP (p =20)	2/0/8	2/1/6	2/3/9	12/0/2	18/4/25
	PPSTAP (p =40)	1/2/7	0/1/8	2/2/10	8/1/5	11/6/30
PPSTAP (p =40)	PPS	2/6/2	2/3/4	6/6/2	4/10/0	14/25/8
	CMOEA/D-TAP	1/2/7	1/4/4	1/13/0	3/7/4	6/26/15
	PPSTAP (p =10)	2/0/8	3/0/6	4/5/5	6/2/6	15/7/25
	PPSTAP (p =20)	4/0/6	4/1/4	5/3/6	6/0/8	19/4/24
	PPSTAP (p =30)	2/1/7	1/0/8	2/2/10	1/8/5	6/11/30

Table 7. Friedman test results for sensitivity analysis (Ref.: PPSTAP, p = 20).

Metric	Competitor	CF	DASCMOP	LIRCMOP	MW	Overall
IGD	PPS	2/6/1	1/2/2	5/7/2	3/7/0	9/24/5
	CMOEA/D-TAP	0/2/7	0/3/2	0/14/0	2/1/7	2/20/16
	PPSTAP (p =10)	0/1/8	0/0/5	0/3/11	0/1/9	0/5/33
	PPSTAP (p =30)	0/0/9	0/0/5	0/0/14	0/3/7	0/3/35
	PPSTAP (p =40)	0/2/7	0/0/5	1/1/12	0/1/9	1/4/33
HV	PPS	2/5/2	1/2/2	5/5/4	3/6/1	11/18/9
	CMOEA/D-TAP	0/2/7	0/4/1	0/14/0	1/5/4	1/25/12
	PPSTAP (p =10)	0/1/8	0/1/4	1/2/11	0/1/9	1/5/32
	PPSTAP (p =30)	0/0/9	0/0/5	0/0/14	0/5/5	0/5/33
	PPSTAP (p =40)	0/2/7	0/0/5	0/1/13	0/2/8	0/5/33
IGDp	PPS	2/6/1	1/2/2	5/8/1	3/7/0	11/23/4
	CMOEA/D-TAP	0/2/7	0/4/1	0/14/0	1/4/5	1/24/13
	PPSTAP (p =10)	0/1/8	0/0/5	1/4/9	0/1/9	1/6/31
	PPSTAP (p =30)	0/0/9	0/0/5	0/0/14	0/5/5	0/5/33
	PPSTAP (p =40)	0/2/7	0/0/5	0/2/12	0/3/7	0/7/31

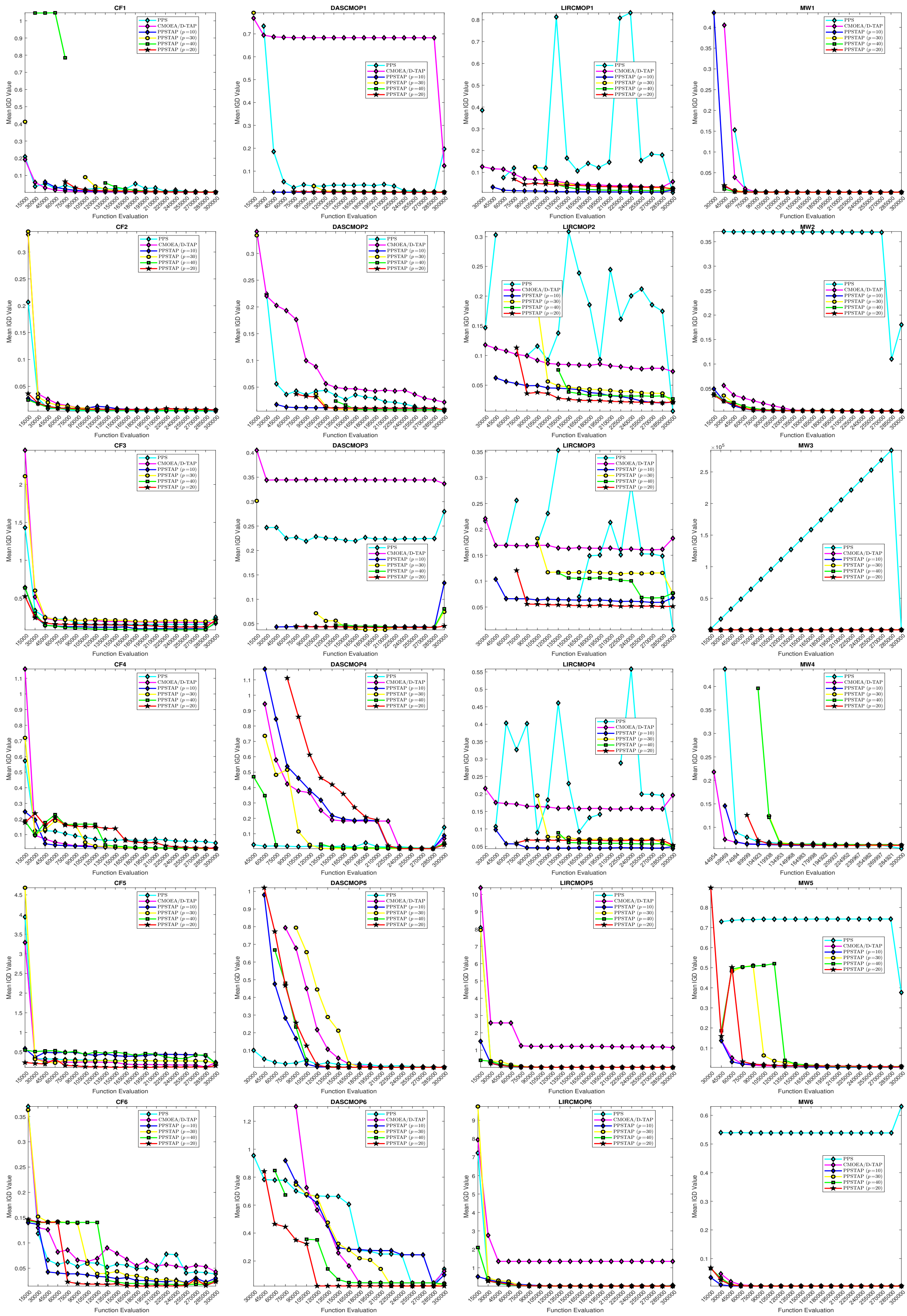

Figure 2. Mean IGD convergence profiles for sensitively analysis.

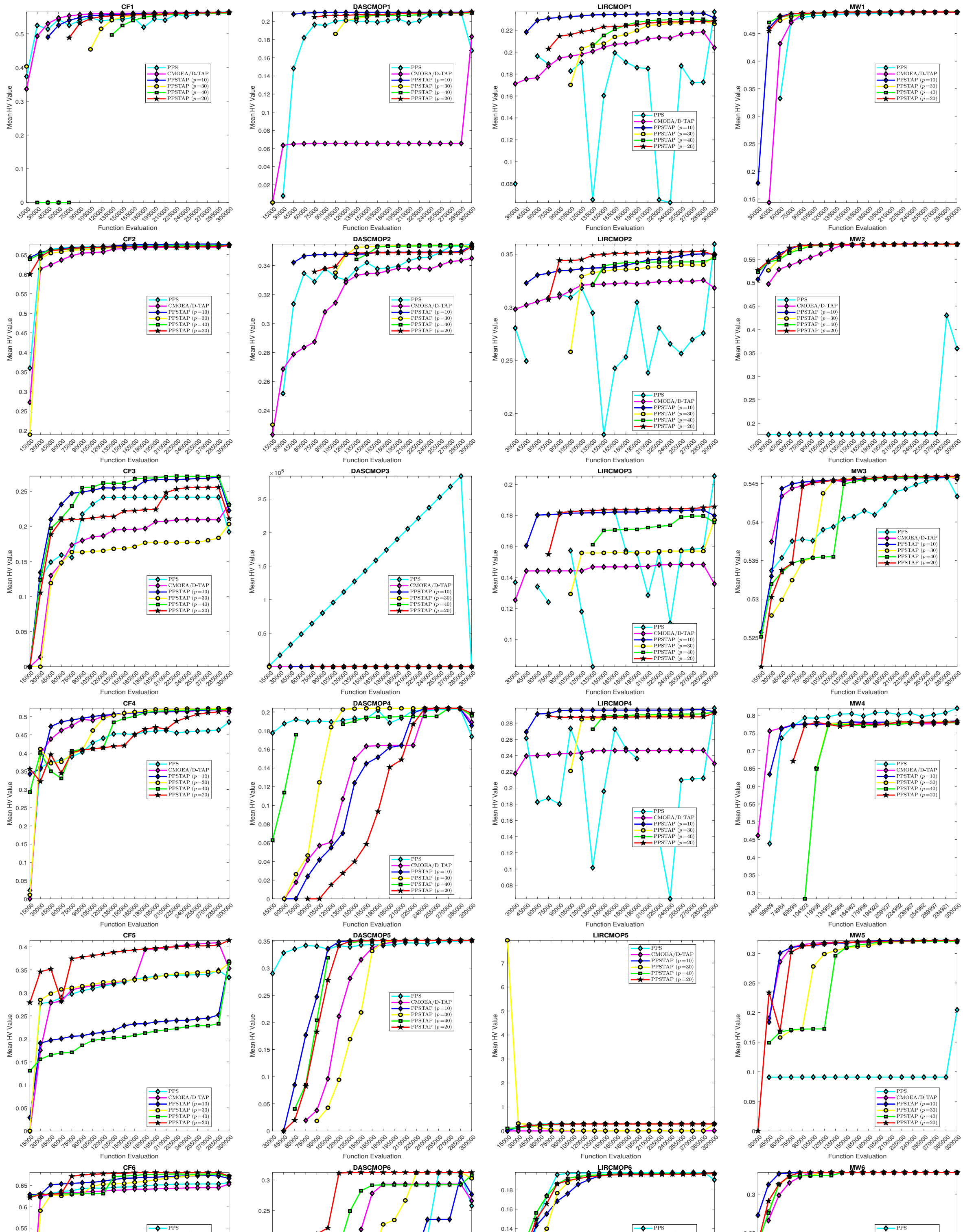

Figure 3. Mean HV convergence profiles for sensitively analysis.

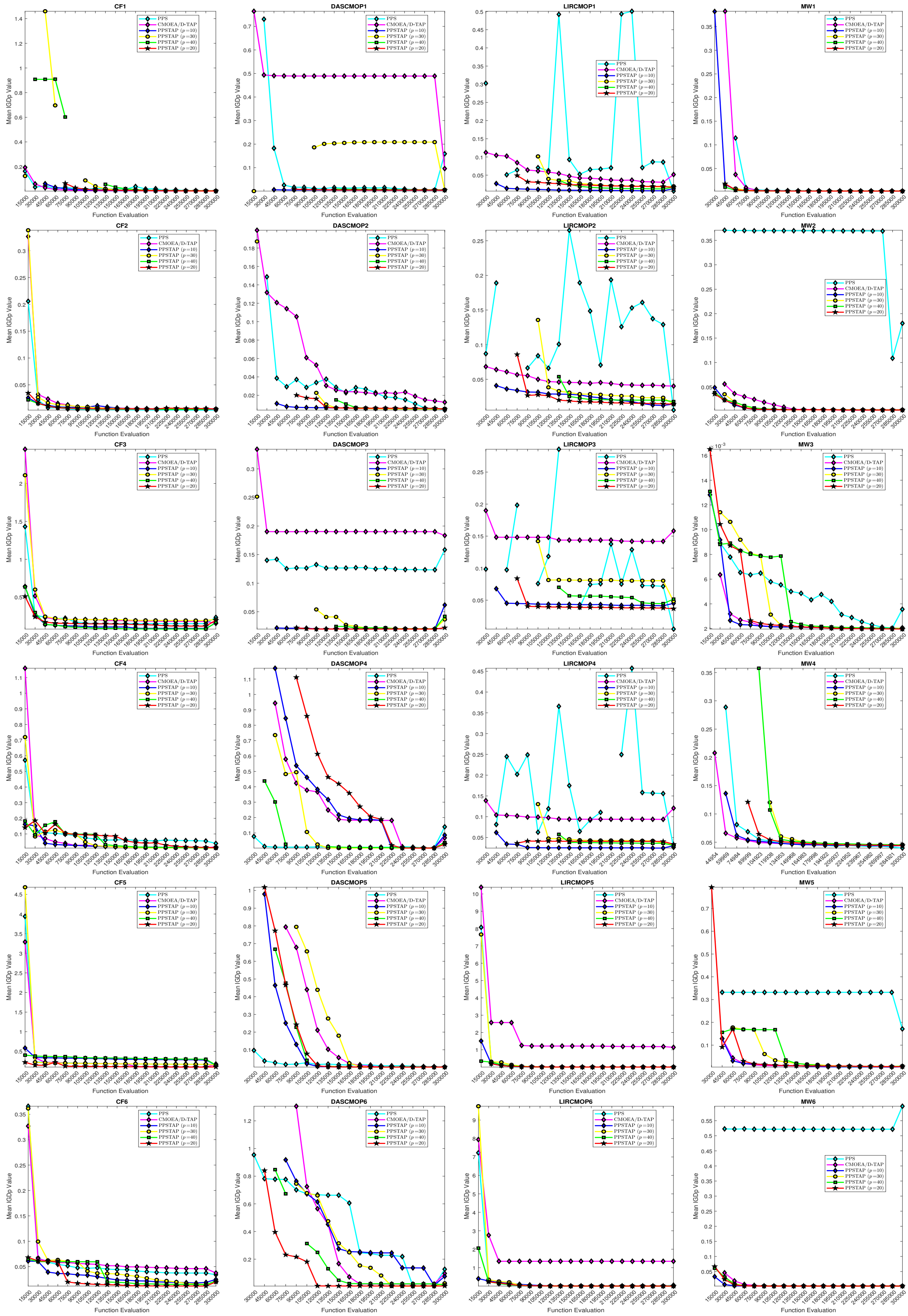

Figure 4. Mean IGDp convergence profiles for sensitively analysis.

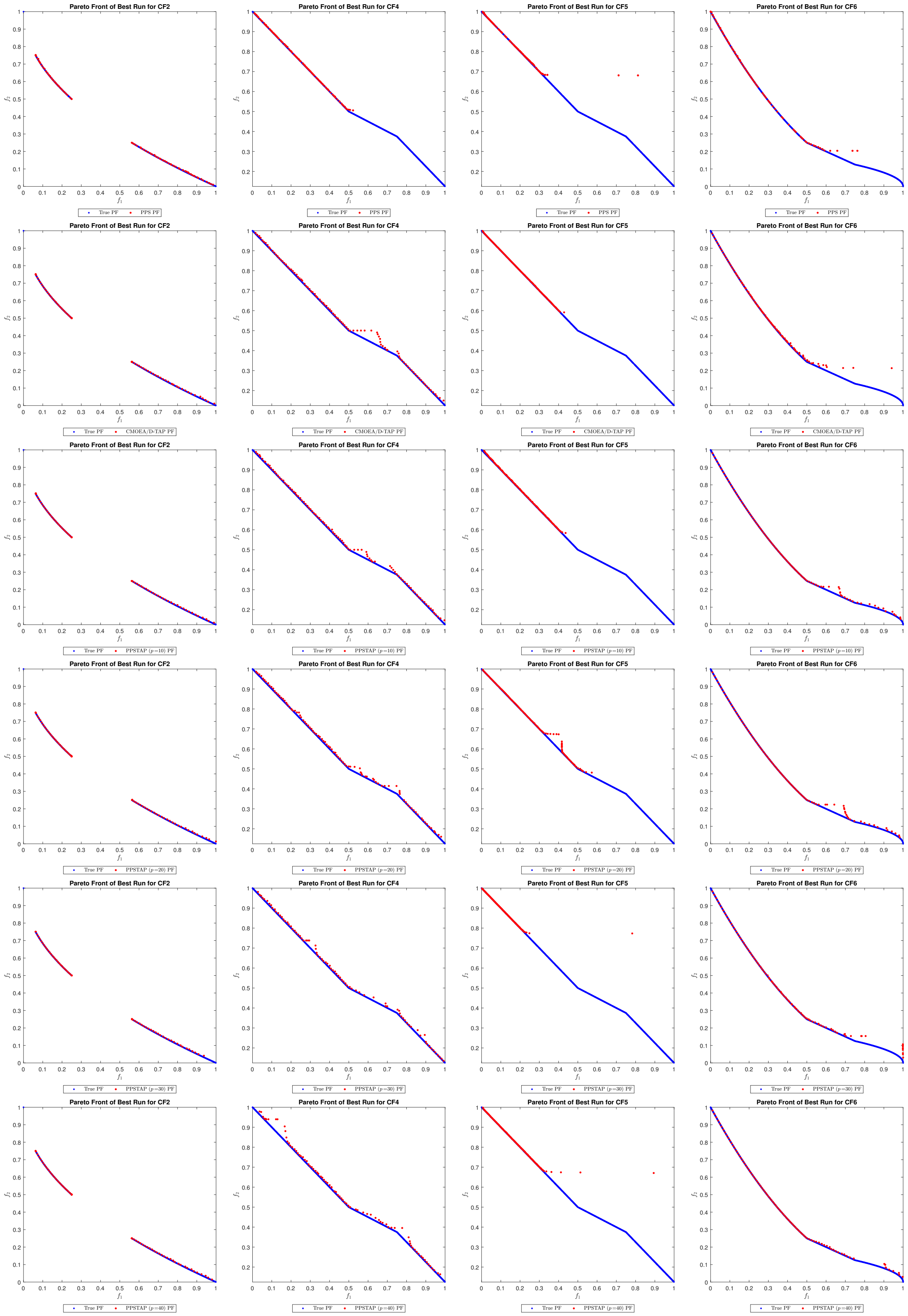

Figure 5. Best pareto fronts for selected CF problems in the sensitivity analysis.

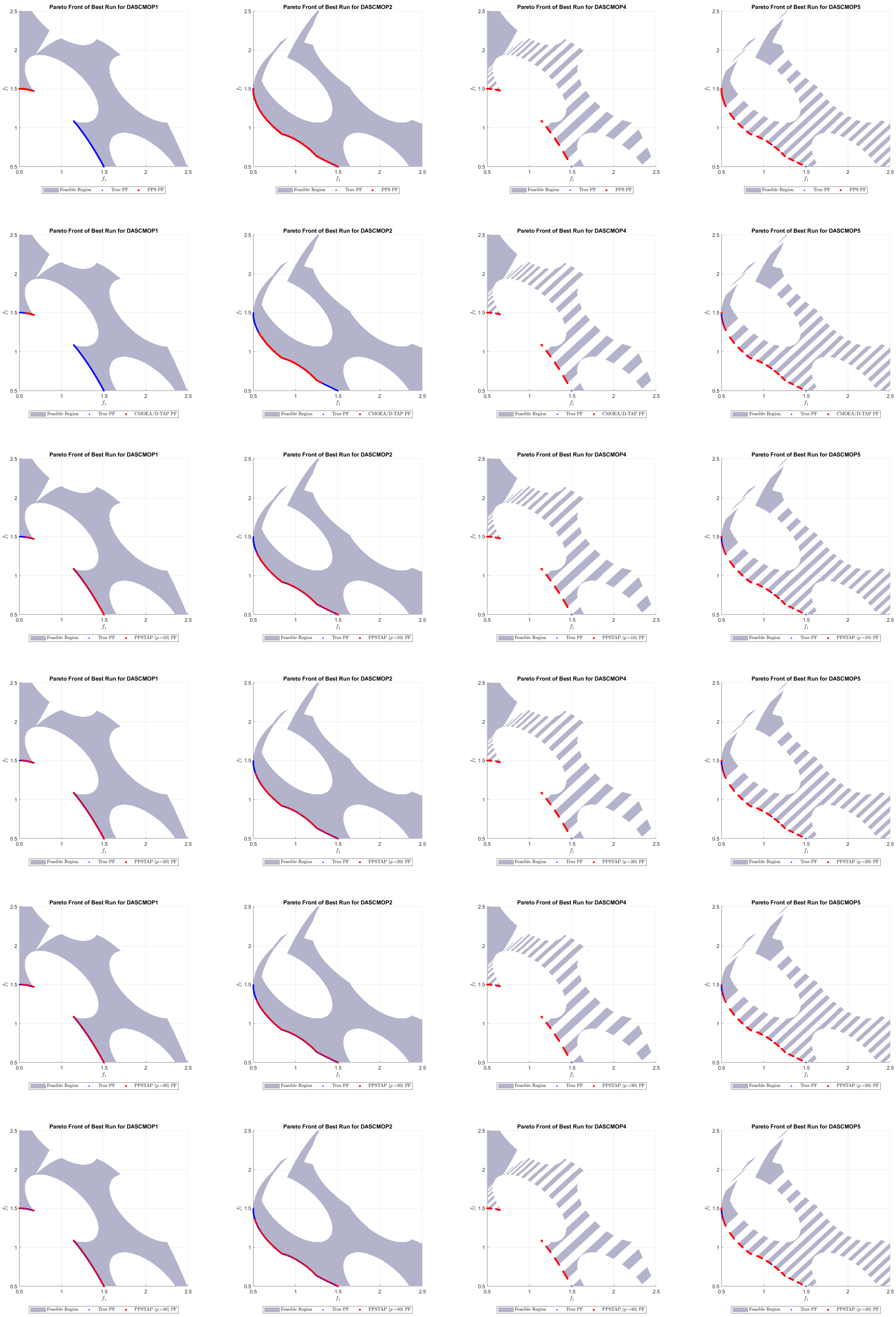

Figure 6. Best pareto fronts for selected DASCMOP problems in the sensitivity analysis.

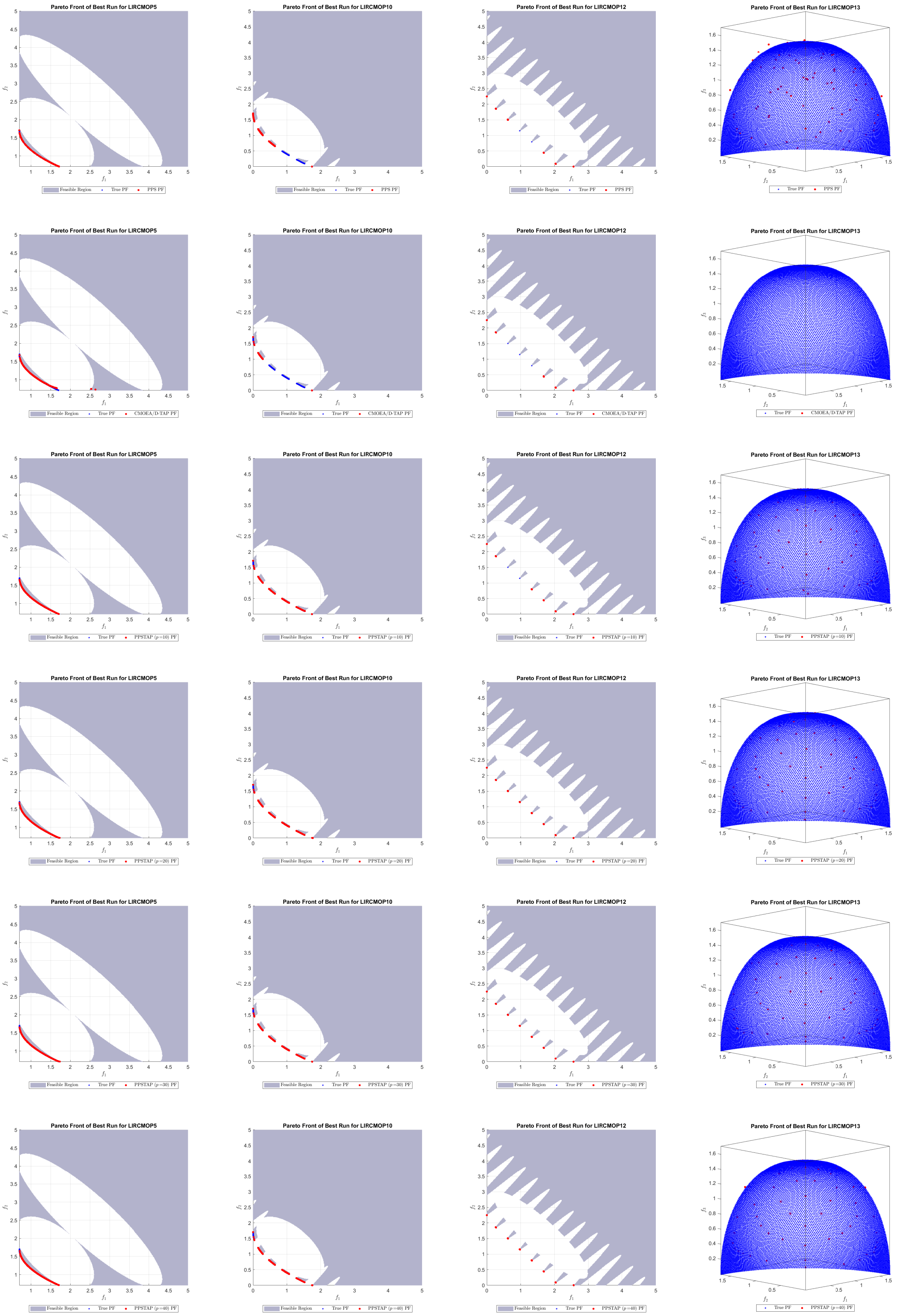

Figure 7. Best pareto fronts for selected LIRCMOP problems in the sensitivity analysis.

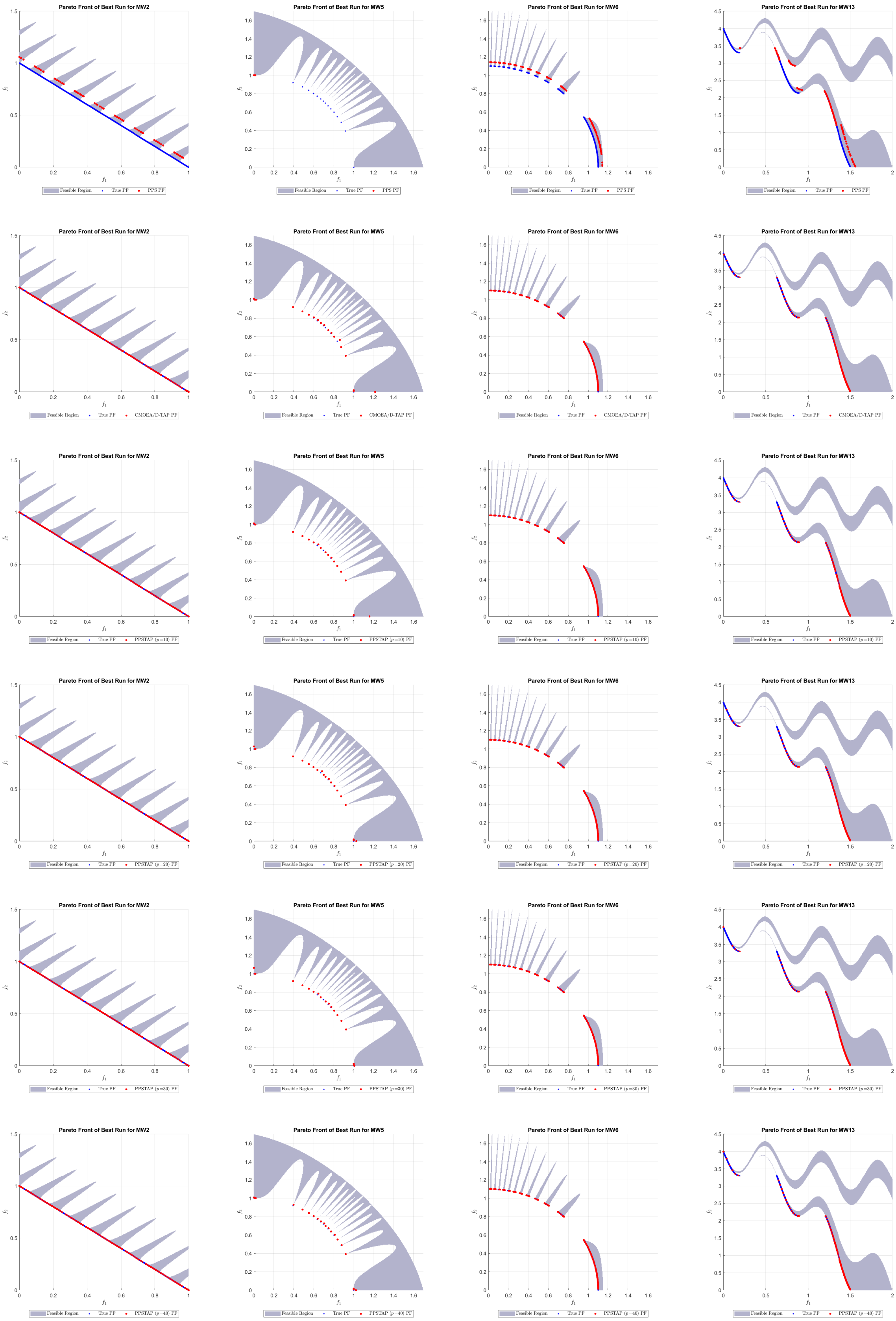

Figure 8. Best pareto fronts for selected MW problems in the sensitivity analysis.

Table 8. Mean and standard deviation of IGD values for comparative analysis.

Problem	M	D	BiCo	C3M	CCMO	PPSTAP (p =30)
CF1	2	10	6.8463e-3 (1.18e-3)	3.6429e-4 (2.00e-4)	2.2975e-3 (3.22e-4)	2.2580e-3 (4.84e-4)
CF2	2	10	3.1851e-2 (1.36e-2)	3.5914e-3 (5.67e-4)	1.6922e-2 (8.75e-3)	5.2311e-3 (4.82e-4)
CF3	2	10	2.3673e-1 (1.07e-1)	2.0338e-1 (7.39e-2)	2.4348e-1 (9.44e-2)	2.1044e-1 (1.18e-1)
CF4	2	10	8.7212e-2 (3.84e-2)	2.9350e-2 (6.66e-3)	7.9088e-2 (3.15e-2)	1.2080e-2 (2.25e-3)
CF5	2	10	3.3659e-1 (1.29e-1)	1.3031e-1 (4.95e-2)	2.6459e-1 (1.30e-1)	1.3855e-1 (7.92e-2)
CF6	2	10	7.9314e-2 (3.30e-2)	2.5701e-2 (4.00e-3)	4.4236e-2 (1.78e-2)	2.3311e-2 (1.15e-2)
CF7	2	10	3.0262e-1 (1.37e-1)	8.1436e-2 (2.20e-2)	2.3030e-1 (1.02e-1)	1.6582e-1 (9.30e-2)
CF8	3	10	1.9279e-1 (9.67e-2)	3.7148e-1 (1.12e-1)	1.9395e-1 (7.94e-2)	1.3062e-1 (8.28e-3)
CF9	3	10	9.1047e-2 (4.38e-3)	1.9180e-1 (3.91e-2)	9.9446e-2 (2.45e-2)	8.4495e-2 (3.08e-3)
CF10	3	10	3.7129e-1 (1.36e-1)	5.0558e-1 (9.86e-2)	3.4167e-1 (5.63e-2)	1.7664e-1 (4.01e-2)
DASCMOP1	2	30	7.1116e-1 (4.10e-2)	3.2910e-3 (8.39e-4)	7.0289e-1 (3.47e-2)	7.5893e-3 (7.39e-4)
DASCMOP2	2	30	2.2728e-1 (2.26e-2)	4.1425e-3 (7.07e-5)	2.3733e-1 (2.60e-2)	7.7942e-3 (1.35e-3)
DASCMOP3	2	30	2.8483e-1 (5.44e-2)	6.7290e-2 (8.29e-2)	3.3004e-1 (5.06e-2)	4.5343e-2 (1.98e-2)
DASCMOP4	2	30	1.3812e-3 (4.35e-4)	1.7357e-3 (1.13e-3)	1.2515e-3 (5.22e-4)	2.7497e-2 (6.17e-2)
DASCMOP5	2	30	2.7248e-3 (7.22e-5)	2.9031e-2 (1.41e-1)	2.7185e-3 (4.95e-5)	4.3719e-3 (1.80e-4)
DASCMOP6	2	30	1.5576e-2 (5.67e-3)	6.9841e-2 (1.94e-1)	2.0488e-2 (5.92e-3)	2.0588e-2 (2.28e-3)
DASCMOP7	3	30	3.1563e-2 (9.70e-4)	4.2655e-2 (8.37e-3)	3.1020e-2 (6.01e-4)	1.0421e-1 (7.11e-2)
DASCMOP8	3	30	4.0745e-2 (9.82e-4)	5.1953e-2 (1.16e-2)	4.0172e-2 (9.22e-4)	9.8559e-2 (4.95e-2)
DASCMOP9	3	30	2.9696e-1 (5.24e-2)	4.1368e-2 (8.46e-4)	3.3365e-1 (8.08e-2)	1.3239e-1 (5.98e-3)
LIRCMOP1	2	30	1.7727e-1 (1.55e-2)	6.3130e-2 (4.53e-2)	1.8712e-1 (6.30e-2)	2.2850e-2 (1.32e-2)
LIRCMOP2	2	30	1.4522e-1 (1.78e-2)	2.1457e-2 (2.06e-2)	1.6236e-1 (4.00e-2)	2.1454e-2 (8.65e-3)
LIRCMOP3	2	30	1.9578e-1 (2.46e-2)	1.2423e-1 (1.07e-1)	1.9146e-1 (6.02e-2)	5.1342e-2 (1.51e-2)
LIRCMOP4	2	30	1.9405e-1 (2.47e-2)	1.0137e-1 (9.50e-2)	2.1931e-1 (4.87e-2)	5.3675e-2 (2.14e-2)
LIRCMOP5	2	30	1.2150e+0 (6.68e-3)	8.4653e-3 (2.33e-3)	2.7595e-1 (5.43e-2)	4.4899e-3 (1.59e-4)
LIRCMOP6	2	30	1.3196e+0 (1.41e-1)	6.6562e-3 (5.31e-4)	2.6869e-1 (6.69e-2)	4.1978e-3 (1.68e-4)
LIRCMOP7	2	30	3.3227e-1 (5.39e-1)	7.7581e-3 (8.00e-4)	1.1566e-1 (3.99e-2)	8.5001e-3 (2.42e-3)
LIRCMOP8	2	30	9.9182e-1 (7.50e-1)	7.3763e-3 (3.23e-4)	1.4635e-1 (4.48e-2)	7.8578e-3 (9.06e-4)
LIRCMOP9	2	30	8.7431e-1 (1.13e-1)	1.8803e-1 (1.27e-1)	3.7130e-1 (1.38e-1)	2.6500e-2 (3.83e-2)
LIRCMOP10	2	30	8.7110e-1 (6.18e-2)	1.5117e-1 (1.22e-1)	7.2003e-2 (3.53e-2)	7.1309e-3 (1.74e-4)
LIRCMOP11	2	30	3.9583e-1 (1.99e-1)	6.6375e-2 (7.15e-2)	3.9110e-2 (3.48e-2)	1.7413e-1 (1.11e-1)
LIRCMOP12	2	30	2.8823e-1 (1.96e-1)	7.5018e-2 (7.74e-2)	1.2979e-1 (6.52e-2)	7.4638e-3 (3.93e-3)
LIRCMOP13	3	30	1.3198e+0 (2.41e-3)	1.2841e-1 (5.07e-2)	9.3516e-2 (1.28e-3)	1.3546e-1 (1.19e-3)
LIRCMOP14	3	30	1.2360e+0 (2.15e-1)	1.0249e-1 (1.11e-3)	9.5779e-2 (1.11e-3)	1.4093e-1 (4.10e-3)
MW1	2	15	1.6165e-3 (1.25e-5)	1.8878e-3 (6.73e-5)	1.6190e-3 (1.79e-5)	3.1980e-3 (2.54e-5)
MW2	2	15	1.4268e-2 (6.97e-3)	8.5495e-2 (3.93e-2)	1.8793e-2 (7.77e-3)	3.9859e-3 (3.15e-5)
MW3	2	15	4.6542e-3 (1.52e-4)	4.9254e-3 (1.68e-4)	4.5621e-3 (1.32e-4)	4.1948e-3 (1.02e-4)
MW4	3	15	4.1091e-2 (4.11e-4)	4.8724e-2 (1.22e-3)	4.0682e-2 (3.77e-4)	6.1642e-2 (6.55e-4)
MW5	2	15	6.1497e-4 (4.50e-4)	4.9004e-3 (2.36e-3)	6.5768e-4 (5.79e-4)	5.8625e-3 (2.06e-3)
MW6	2	15	9.3699e-3 (6.42e-3)	3.4660e-1 (2.18e-1)	3.3519e-2 (8.84e-2)	3.9500e-3 (8.32e-6)
MW7	2	15	4.3167e-3 (2.60e-4)	4.6713e-3 (2.75e-4)	4.0874e-3 (1.65e-4)	4.6776e-3 (8.20e-5)
MW8	3	15	4.4829e-2 (1.24e-3)	1.1704e-1 (4.35e-2)	4.4988e-2 (2.48e-3)	6.8520e-2 (1.26e-3)
MW9	2	15	4.6300e-3 (3.26e-4)	3.3350e-2 (1.28e-1)	4.1616e-3 (8.43e-5)	4.8093e-3 (4.56e-4)
MW10	2	15	3.9812e-2 (4.95e-2)	3.3504e-1 (1.89e-1)	3.8576e-2 (3.29e-2)	4.4420e-3 (4.93e-5)
MW11	2	15	5.9169e-3 (1.27e-4)	6.2961e-3 (1.42e-4)	5.9398e-3 (1.31e-4)	1.1324e-2 (9.06e-4)
MW12	2	15	4.6125e-3 (9.45e-5)	3.2990e-2 (1.09e-1)	4.6450e-3 (1.02e-4)	4.9377e-3 (3.98e-5)
MW13	2	15	2.8978e-2 (1.93e-2)	2.1214e-1 (9.03e-2)	5.7187e-2 (3.47e-2)	2.3025e-2 (3.74e-3)
MW14	3	15	9.8157e-2 (2.02e-3)	1.0285e-1 (1.95e-3)	9.7594e-2 (1.80e-3)	3.6034e-1 (3.08e-2)

Table 9. Mean and standard deviation of HV values for comparative analysis.

Problem	M	D	BiCo	C3M	CCMO	PPSTAP (p =30)
CF1	2	10	5.5724e-1 (1.57e-3)	5.6567e-1 (2.44e-4)	5.6327e-1 (3.97e-4)	5.6291e-1 (6.82e-4)
CF2	2	10	6.3778e-1 (2.21e-2)	6.7652e-1 (6.47e-4)	6.6099e-1 (1.30e-2)	6.7419e-1 (1.55e-3)
CF3	2	10	2.0446e-1 (4.50e-2)	1.7607e-1 (5.03e-2)	2.0126e-1 (3.71e-2)	2.1117e-1 (5.12e-2)
CF4	2	10	4.3120e-1 (2.35e-2)	4.9651e-1 (9.38e-3)	4.3997e-1 (2.59e-2)	5.1957e-1 (3.92e-3)
CF5	2	10	2.6455e-1 (6.67e-2)	3.6917e-1 (5.31e-2)	2.9202e-1 (7.21e-2)	4.2144e-1 (4.54e-2)
CF6	2	10	6.4078e-1 (1.54e-2)	6.7878e-1 (2.93e-3)	6.6308e-1 (1.31e-2)	6.7229e-1 (1.17e-2)
CF7	2	10	4.5402e-1 (8.99e-2)	5.9091e-1 (2.59e-2)	4.8380e-1 (8.41e-2)	5.1416e-1 (9.45e-2)
CF8	3	10	3.4091e-1 (8.61e-2)	1.3961e-1 (5.60e-2)	3.2166e-1 (8.39e-2)	3.9787e-1 (1.08e-2)
CF9	3	10	4.4033e-1 (1.09e-2)	2.9581e-1 (4.94e-2)	4.2522e-1 (3.41e-2)	4.5286e-1 (8.26e-3)
CF10	3	10	1.7655e-1 (6.75e-2)	7.2886e-2 (4.48e-2)	1.6121e-1 (3.64e-2)	2.8381e-1 (4.31e-2)
DASCMOP1	2	30	1.0719e-2 (7.37e-3)	2.1262e-1 (4.58e-4)	1.3389e-2 (1.16e-2)	2.1053e-1 (1.23e-3)
DASCMOP2	2	30	2.5672e-1 (4.02e-3)	3.5535e-1 (6.05e-5)	2.6135e-1 (3.02e-3)	3.5291e-1 (1.87e-3)
DASCMOP3	2	30	2.1947e-1 (1.38e-2)	3.0166e-1 (2.02e-2)	2.1715e-1 (1.69e-2)	2.9330e-1 (7.20e-3)
DASCMOP4	2	30	2.0401e-1 (4.15e-4)	2.0333e-1 (2.24e-3)	2.0403e-1 (1.54e-3)	1.9868e-1 (1.38e-2)
DASCMOP5	2	30	3.5168e-1 (1.06e-4)	3.3989e-1 (5.92e-2)	3.5173e-1 (5.83e-5)	3.5118e-1 (1.16e-4)
DASCMOP6	2	30	3.1164e-1 (3.44e-3)	2.9147e-1 (7.68e-2)	3.0970e-1 (6.56e-3)	3.1232e-1 (2.58e-4)
DASCMOP7	3	30	2.8791e-1 (5.30e-4)	2.7929e-1 (3.85e-3)	2.8895e-1 (2.83e-4)	2.5066e-1 (3.89e-2)
DASCMOP8	3	30	2.0684e-1 (4.45e-4)	1.9865e-1 (4.01e-3)	2.0760e-1 (3.46e-4)	1.7691e-1 (3.49e-2)
DASCMOP9	3	30	1.3877e-1 (1.02e-2)	2.0533e-1 (3.35e-4)	1.3615e-1 (1.54e-2)	1.8307e-1 (2.32e-3)
LIRCMOP1	2	30	1.5124e-1 (7.01e-3)	2.0465e-1 (2.29e-2)	1.5072e-1 (2.04e-2)	2.2841e-1 (6.74e-3)
LIRCMOP2	2	30	2.7871e-1 (1.10e-2)	3.5061e-1 (1.31e-2)	2.7508e-1 (2.01e-2)	3.4918e-1 (6.36e-3)
LIRCMOP3	2	30	1.3325e-1 (8.63e-3)	1.6352e-1 (2.65e-2)	1.3572e-1 (2.13e-2)	1.8558e-1 (7.34e-3)
LIRCMOP4	2	30	2.3045e-1 (1.23e-2)	2.7431e-1 (3.62e-2)	2.2565e-1 (2.22e-2)	2.9240e-1 (1.06e-2)
LIRCMOP5	2	30	0.0000e+0 (0.00e+0)	2.8981e-1 (1.67e-3)	1.6251e-1 (2.04e-2)	2.9132e-1 (3.69e-4)
LIRCMOP6	2	30	2.8842e-3 (1.58e-2)	1.9633e-1 (2.99e-4)	1.2355e-1 (1.14e-2)	1.9687e-1 (2.44e-4)
LIRCMOP7	2	30	2.1344e-1 (8.54e-2)	2.9406e-1 (3.50e-4)	2.4957e-1 (1.22e-2)	2.9161e-1 (1.98e-3)
LIRCMOP8	2	30	1.0642e-1 (1.16e-1)	2.9425e-1 (1.70e-4)	2.4317e-1 (1.08e-2)	2.9225e-1 (9.81e-4)
LIRCMOP9	2	30	1.6337e-1 (6.50e-2)	4.7840e-1 (5.90e-2)	4.3123e-1 (6.65e-2)	5.6016e-1 (1.10e-2)
LIRCMOP10	2	30	9.0855e-2 (2.87e-2)	6.3707e-1 (6.09e-2)	6.7483e-1 (1.30e-2)	7.0603e-1 (4.79e-4)
LIRCMOP11	2	30	4.5020e-1 (1.42e-1)	6.5545e-1 (4.79e-2)	6.7520e-1 (1.81e-2)	6.2669e-1 (4.61e-2)
LIRCMOP12	2	30	4.9588e-1 (8.84e-2)	5.8423e-1 (3.94e-2)	5.5967e-1 (3.72e-2)	6.1962e-1 (1.95e-3)
LIRCMOP13	3	30	6.6420e-5 (1.02e-4)	5.0132e-1 (4.49e-2)	5.5458e-1 (1.37e-3)	4.8629e-1 (4.82e-3)
LIRCMOP14	3	30	1.9008e-2 (1.01e-1)	5.3957e-1 (2.08e-3)	5.5392e-1 (1.17e-3)	4.9361e-1 (5.52e-3)
MW1	2	15	4.9013e-1 (1.41e-5)	4.8906e-1 (2.46e-4)	4.9013e-1 (1.11e-5)	4.8880e-1 (3.82e-4)
MW2	2	15	5.6395e-1 (1.21e-2)	4.6438e-1 (5.07e-2)	5.5642e-1 (1.25e-2)	5.8212e-1 (3.69e-5)
MW3	2	15	5.4453e-1 (3.95e-4)	5.4374e-1 (2.91e-4)	5.4495e-1 (2.80e-4)	5.4596e-1 (1.07e-4)
MW4	3	15	8.4120e-1 (6.97e-4)	8.2747e-1 (1.51e-3)	8.4186e-1 (3.48e-4)	7.8169e-1 (3.58e-3)
MW5	2	15	3.2433e-1 (2.67e-4)	3.2057e-1 (2.20e-3)	3.2440e-1 (2.34e-4)	3.2145e-1 (1.02e-3)
MW6	2	15	3.1808e-1 (9.73e-3)	1.5869e-1 (7.38e-2)	3.0001e-1 (3.67e-2)	3.2778e-1 (1.35e-5)
MW7	2	15	4.1235e-1 (5.84e-4)	4.1197e-1 (2.75e-4)	4.1290e-1 (2.54e-4)	4.1225e-1 (1.33e-4)
MW8	3	15	5.4379e-1 (7.65e-3)	3.8828e-1 (7.46e-2)	5.3603e-1 (9.31e-3)	4.9080e-1 (8.08e-3)
MW9	2	15	3.9656e-1 (2.01e-3)	3.7287e-1 (7.07e-2)	4.0057e-1 (1.26e-3)	3.9757e-1 (1.87e-3)
MW10	2	15	4.1926e-1 (3.37e-2)	2.5393e-1 (8.78e-2)	4.1813e-1 (2.38e-2)	4.5422e-1 (2.57e-4)
MW11	2	15	4.4808e-1 (1.30e-4)	4.4742e-1 (1.41e-4)	4.4791e-1 (1.68e-4)	4.4561e-1 (1.26e-3)
MW12	2	15	6.0534e-1 (1.07e-4)	5.7471e-1 (1.03e-1)	6.0510e-1 (2.09e-4)	6.0465e-1 (1.05e-4)
MW13	2	15	4.6466e-1 (9.31e-3)	3.5476e-1 (5.29e-2)	4.5134e-1 (1.59e-2)	4.7356e-1 (1.34e-3)
MW14	3	15	4.6992e-1 (1.58e-3)	4.6393e-1 (1.82e-3)	4.7379e-1 (1.48e-3)	3.9764e-1 (8.39e-3)

Table 10. Mean and standard deviation of IGDp values for comparative analysis.

Problem	M	D	BiCo	C3M	CCMO	PPSTAP (p =30)
CF1	2	10	6.8463e-3 (1.18e-3)	3.6429e-4 (2.00e-4)	2.2975e-3 (3.22e-4)	2.2580e-3 (4.84e-4)
CF2	2	10	2.5149e-2 (1.01e-2)	3.3346e-3 (5.64e-4)	1.3544e-2 (6.06e-3)	4.4395e-3 (4.63e-4)
CF3	2	10	1.8177e-1 (5.66e-2)	1.8604e-1 (5.99e-2)	2.0140e-1 (7.46e-2)	1.9605e-1 (1.09e-1)
CF4	2	10	6.7777e-2 (2.09e-2)	2.6967e-2 (5.79e-3)	6.2474e-2 (2.16e-2)	1.1236e-2 (2.05e-3)
CF5	2	10	2.3752e-1 (8.75e-2)	1.2142e-1 (4.80e-2)	1.9415e-1 (9.01e-2)	9.5598e-2 (4.83e-2)
CF6	2	10	4.9650e-2 (1.53e-2)	1.8970e-2 (2.20e-3)	2.8741e-2 (1.25e-2)	1.9997e-2 (1.05e-2)
CF7	2	10	1.9024e-1 (1.07e-1)	6.6993e-2 (1.93e-2)	1.5062e-1 (7.98e-2)	1.2143e-1 (7.07e-2)
CF8	3	10	1.3566e-1 (6.23e-2)	3.2302e-1 (1.18e-1)	1.4684e-1 (6.78e-2)	9.5200e-2 (5.61e-3)
CF9	3	10	5.5906e-2 (3.38e-3)	1.4435e-1 (3.60e-2)	6.3891e-2 (1.48e-2)	6.0356e-2 (2.24e-3)
CF10	3	10	3.0936e-1 (1.77e-1)	4.3735e-1 (9.58e-2)	2.5834e-1 (6.66e-2)	1.5165e-1 (4.27e-2)
DASCMOP1	2	30	7.0802e-1 (3.95e-2)	1.7621e-3 (1.41e-4)	6.9353e-1 (5.08e-2)	4.7031e-3 (9.28e-4)
DASCMOP2	2	30	1.3657e-1 (9.47e-3)	3.1330e-3 (1.05e-4)	1.3809e-1 (9.58e-3)	5.0578e-3 (4.67e-4)
DASCMOP3	2	30	1.7390e-1 (2.51e-2)	2.8804e-2 (4.05e-2)	1.7876e-1 (3.00e-2)	2.2106e-2 (1.22e-2)
DASCMOP4	2	30	7.0570e-4 (1.42e-4)	9.4610e-4 (4.88e-4)	6.7619e-4 (3.10e-4)	2.6050e-2 (6.21e-2)
DASCMOP5	2	30	1.7730e-3 (9.33e-5)	2.8380e-2 (1.41e-1)	1.7104e-3 (4.94e-5)	2.7602e-3 (1.94e-4)
DASCMOP6	2	30	5.7717e-3 (2.54e-3)	5.7531e-2 (1.97e-1)	7.2698e-3 (5.01e-3)	6.2696e-3 (3.70e-4)
DASCMOP7	3	30	2.4578e-2 (1.23e-3)	3.8074e-2 (7.42e-3)	2.2896e-2 (7.01e-4)	9.7183e-2 (7.54e-2)
DASCMOP8	3	30	1.8876e-2 (7.42e-4)	3.1224e-2 (6.91e-3)	1.8949e-2 (9.02e-4)	6.6599e-2 (5.86e-2)
DASCMOP9	3	30	2.1075e-1 (3.15e-2)	1.9691e-2 (8.98e-4)	2.2198e-1 (4.40e-2)	5.4139e-2 (3.33e-3)
LIRCMOP1	2	30	1.5424e-1 (1.25e-2)	5.3869e-2 (4.06e-2)	1.5959e-1 (5.04e-2)	1.6058e-2 (9.48e-3)
LIRCMOP2	2	30	8.6202e-2 (1.27e-2)	1.4072e-2 (1.08e-2)	9.5770e-2 (2.69e-2)	1.4316e-2 (4.77e-3)
LIRCMOP3	2	30	1.6856e-1 (1.92e-2)	9.2064e-2 (7.69e-2)	1.6210e-1 (4.85e-2)	3.6673e-2 (1.19e-2)
LIRCMOP4	2	30	1.1943e-1 (1.86e-2)	6.6595e-2 (6.40e-2)	1.3258e-1 (3.41e-2)	3.3722e-2 (1.26e-2)
LIRCMOP5	2	30	1.2145e+0 (7.33e-3)	8.0351e-3 (1.94e-3)	2.0763e-1 (4.59e-2)	3.4394e-3 (1.75e-4)
LIRCMOP6	2	30	1.3132e+0 (1.75e-1)	6.0404e-3 (5.35e-4)	2.1678e-1 (4.47e-2)	3.2174e-3 (2.23e-4)
LIRCMOP7	2	30	3.1511e-1 (5.45e-1)	6.1569e-3 (7.42e-4)	9.7325e-2 (3.08e-2)	6.6502e-3 (2.33e-3)
LIRCMOP8	2	30	9.7667e-1 (7.66e-1)	5.8077e-3 (3.44e-4)	1.2584e-1 (3.70e-2)	6.0139e-3 (9.04e-4)
LIRCMOP9	2	30	8.0293e-1 (1.51e-1)	1.2702e-1 (7.31e-2)	2.4333e-1 (1.24e-1)	1.7484e-2 (2.64e-2)
LIRCMOP10	2	30	8.2233e-1 (7.64e-2)	1.1535e-1 (9.24e-2)	5.5339e-2 (2.13e-2)	4.9548e-3 (1.74e-4)
LIRCMOP11	2	30	3.4138e-1 (2.10e-1)	5.1348e-2 (5.98e-2)	2.9861e-2 (2.58e-2)	9.9285e-2 (5.98e-2)
LIRCMOP12	2	30	2.4379e-1 (1.78e-1)	5.9912e-2 (6.31e-2)	1.0382e-1 (5.36e-2)	4.8038e-3 (4.00e-3)
LIRCMOP13	3	30	1.3181e+0 (2.35e-3)	1.0174e-1 (5.49e-2)	4.4867e-2 (1.46e-3)	9.1500e-2 (2.57e-3)
LIRCMOP14	3	30	1.2326e+0 (2.24e-1)	6.1468e-2 (2.24e-3)	4.6643e-2 (1.27e-3)	8.8766e-2 (3.44e-3)
MW1	2	15	1.1423e-3 (1.54e-5)	1.7046e-3 (9.31e-5)	1.1420e-3 (1.55e-5)	2.2918e-3 (2.93e-5)
MW2	2	15	1.3359e-2 (7.13e-3)	8.5446e-2 (3.93e-2)	1.7994e-2 (8.02e-3)	2.8184e-3 (2.23e-5)
MW3	2	15	2.8151e-3 (2.06e-4)	3.3245e-3 (1.81e-4)	2.6115e-3 (1.57e-4)	1.9604e-3 (5.14e-5)
MW4	3	15	2.9292e-2 (4.32e-4)	4.1900e-2 (1.45e-3)	2.9045e-2 (3.43e-4)	4.4158e-2 (5.28e-4)
MW5	2	15	6.1121e-4 (4.52e-4)	4.9004e-3 (2.36e-3)	5.9906e-4 (4.57e-4)	5.5174e-3 (1.72e-3)
MW6	2	15	8.6855e-3 (7.07e-3)	3.3375e-1 (2.09e-1)	3.2567e-2 (8.41e-2)	1.8262e-3 (1.52e-5)
MW7	2	15	1.9206e-3 (2.79e-4)	2.2079e-3 (1.05e-4)	1.7363e-3 (1.22e-4)	2.1268e-3 (6.03e-5)
MW8	3	15	2.3721e-2 (4.13e-3)	1.1294e-1 (4.53e-2)	2.7755e-2 (5.27e-3)	4.7605e-2 (3.34e-3)
MW9	2	15	3.0609e-3 (3.60e-4)	3.0138e-2 (1.18e-1)	2.5962e-3 (1.17e-4)	3.2981e-3 (4.43e-4)
MW10	2	15	3.7401e-2 (4.59e-2)	2.9574e-1 (1.52e-1)	3.6545e-2 (3.07e-2)	2.5463e-3 (1.73e-5)
MW11	2	15	2.4488e-3 (1.24e-4)	3.3100e-3 (1.63e-4)	2.5197e-3 (1.40e-4)	4.4143e-3 (3.53e-4)
MW12	2	15	2.6916e-3 (9.49e-5)	3.0370e-2 (1.05e-1)	2.8080e-3 (1.38e-4)	2.8680e-3 (6.44e-5)
MW13	2	15	1.6265e-2 (1.07e-2)	1.9678e-1 (9.44e-2)	3.3324e-2 (2.14e-2)	7.3300e-3 (6.78e-4)
MW14	3	15	6.2221e-2 (1.62e-3)	7.4950e-2 (2.06e-3)	6.3600e-2 (1.58e-3)	1.8427e-1 (1.25e-2)

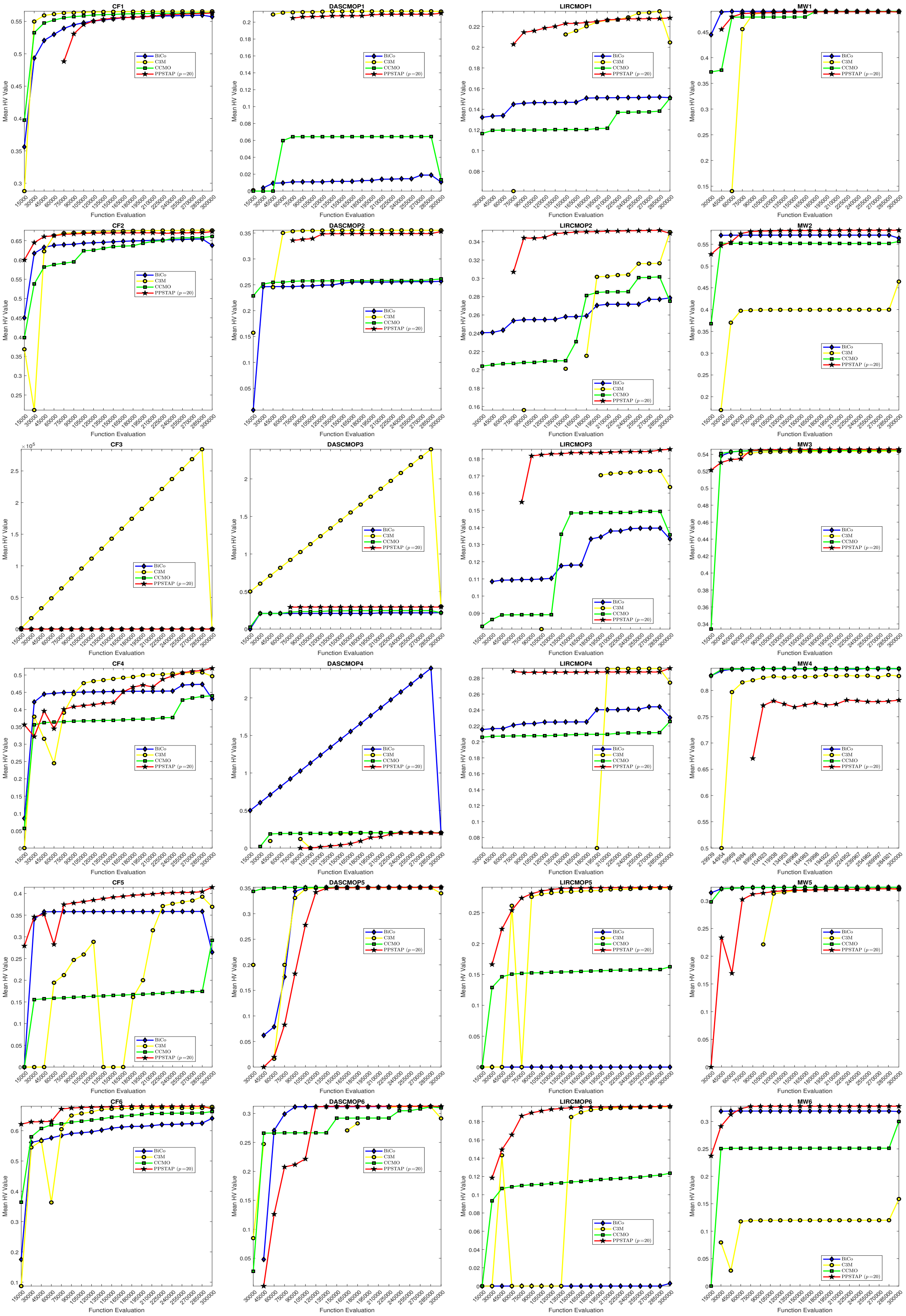

Figure 9. Mean IGD convergence profiles for comparative analysis.

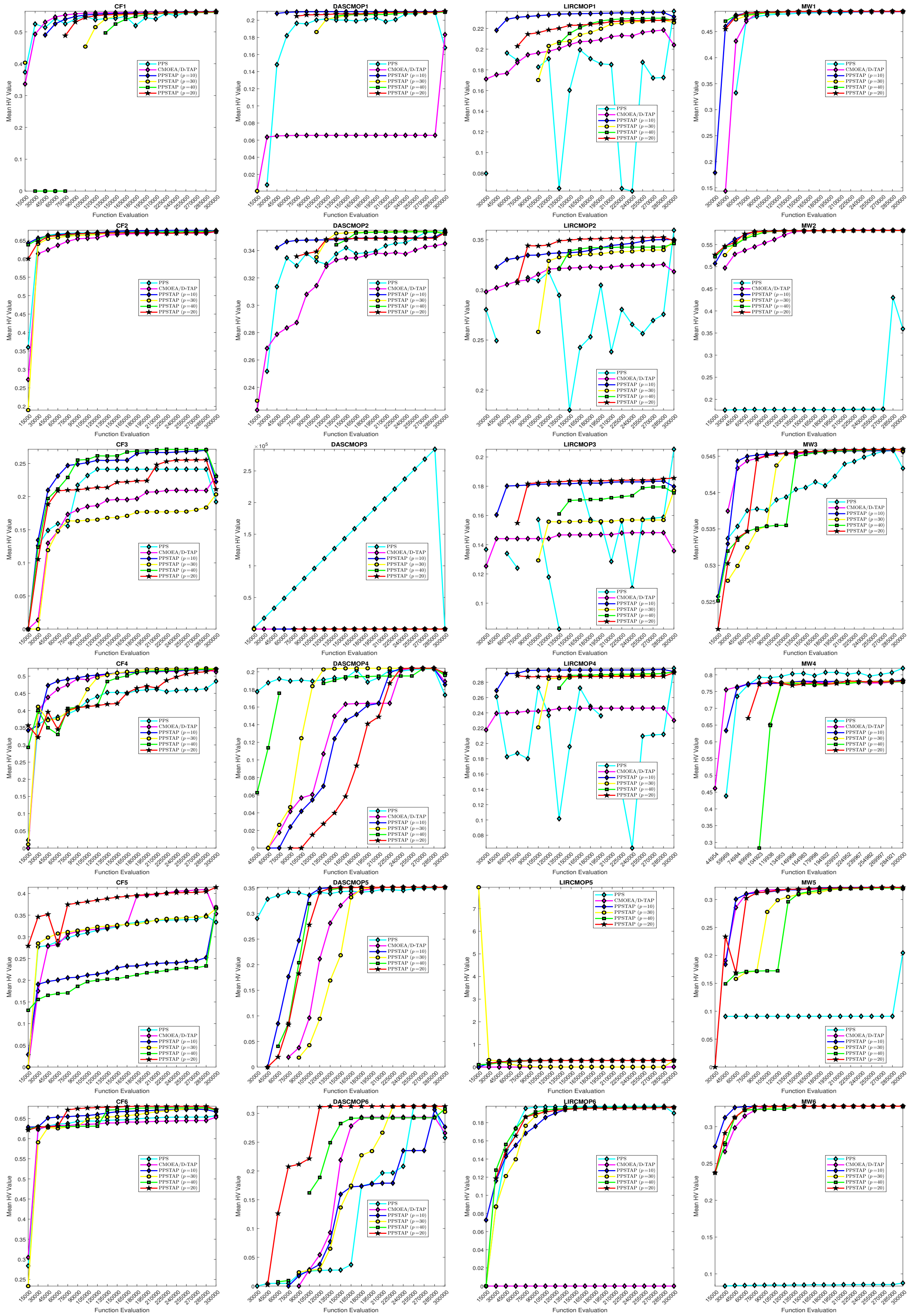

Figure 10. Mean HV convergence profiles for comparative analysis.

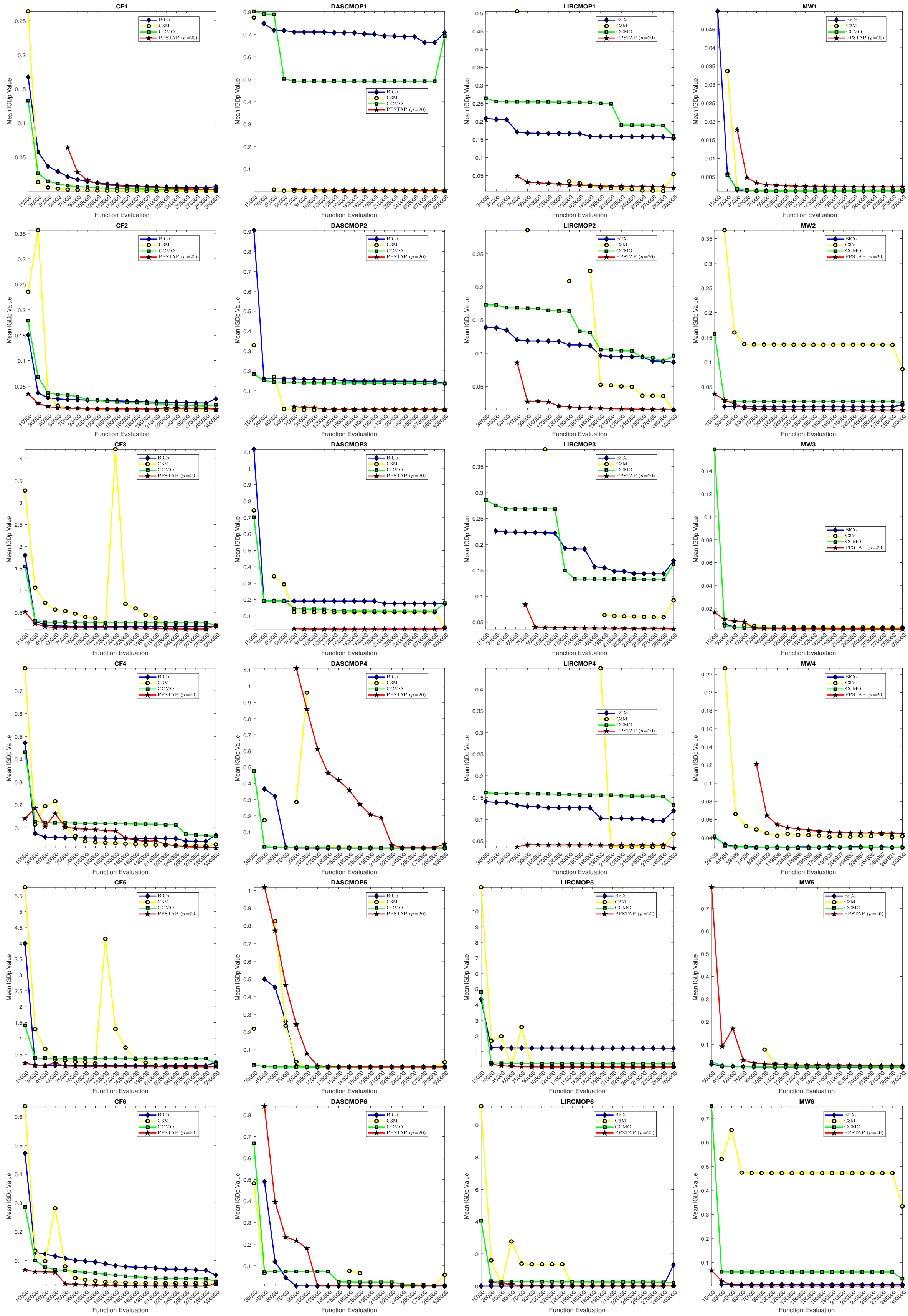

Figure 11. Mean IGDp convergence profiles for comparative analysis.

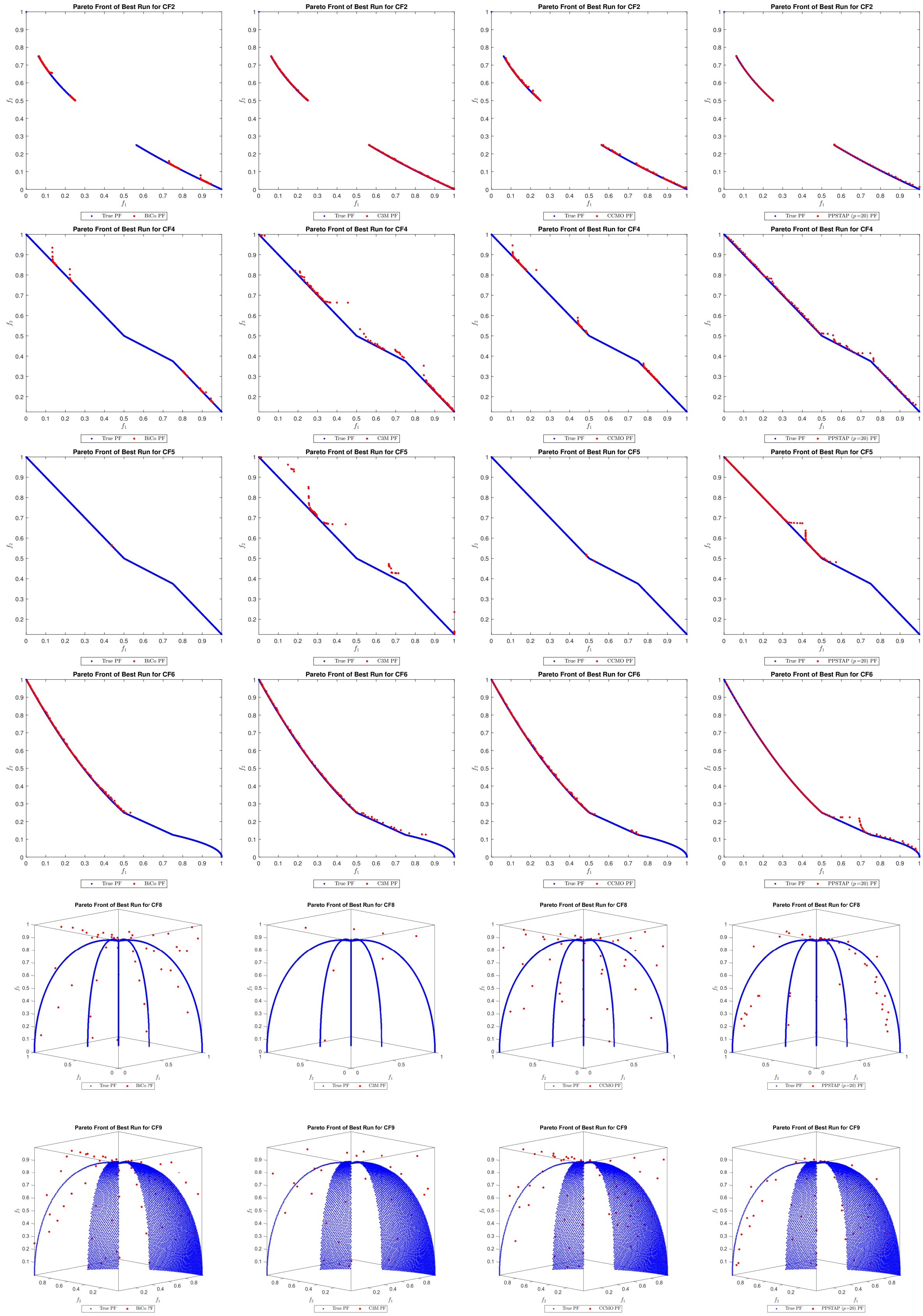

Figure 12. Best pareto fronts for selected CF problems in the sensitivity analysis.

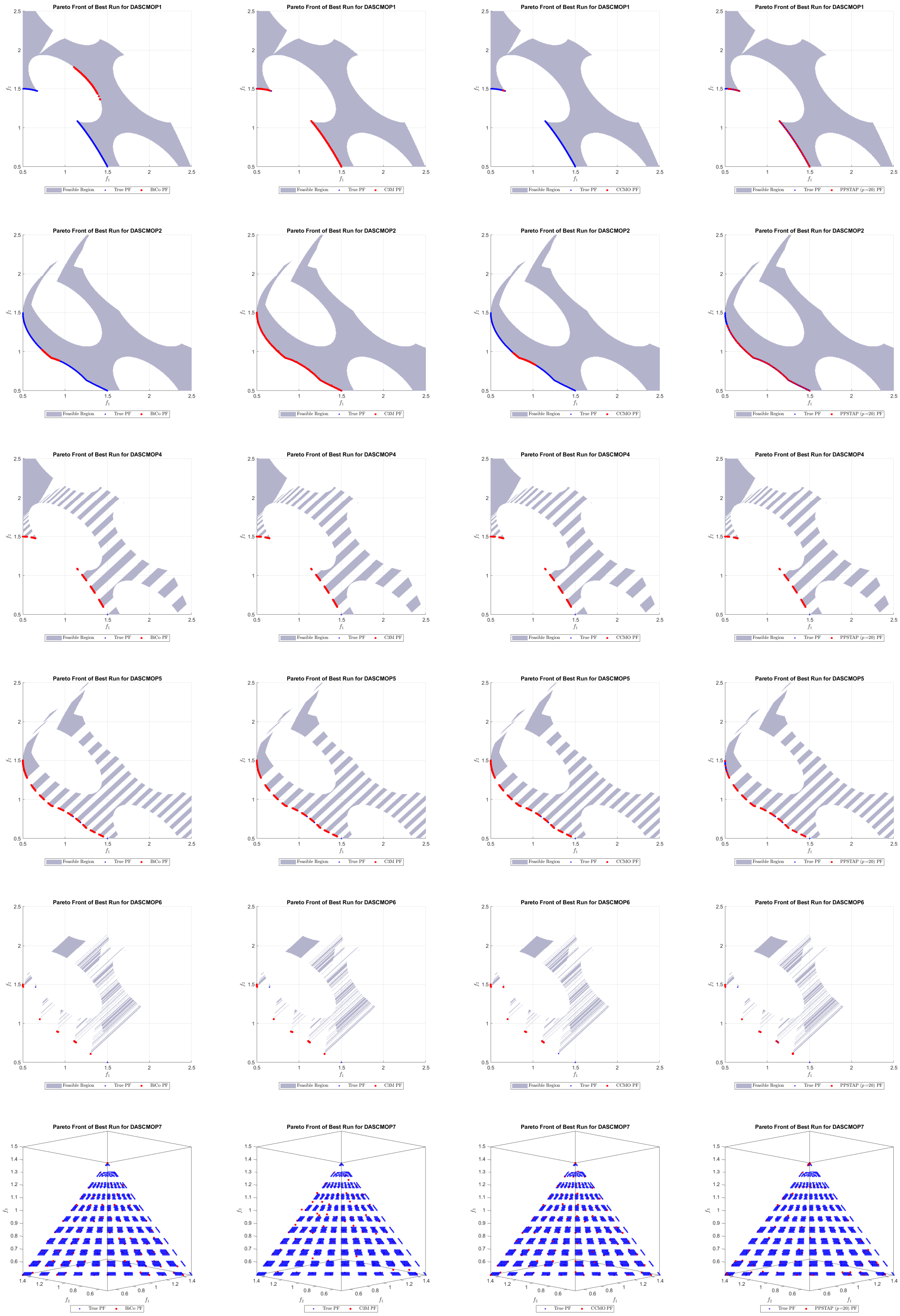

Figure 13. Best pareto fronts for selected DASCMOP problems in the sensitivity analysis.

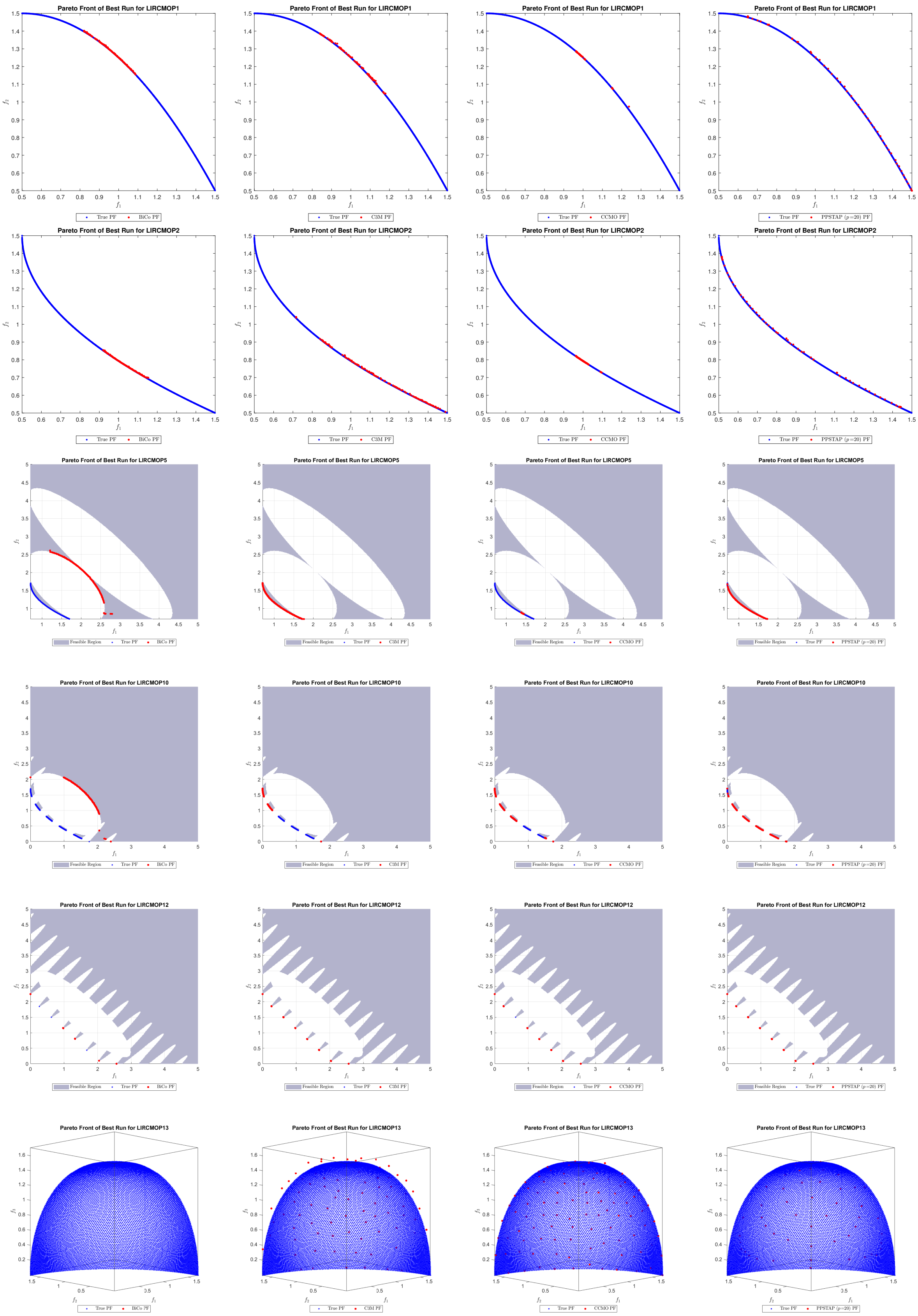

Figure 14. Best pareto fronts for selected LIRCMOP problems in the sensitivity analysis.

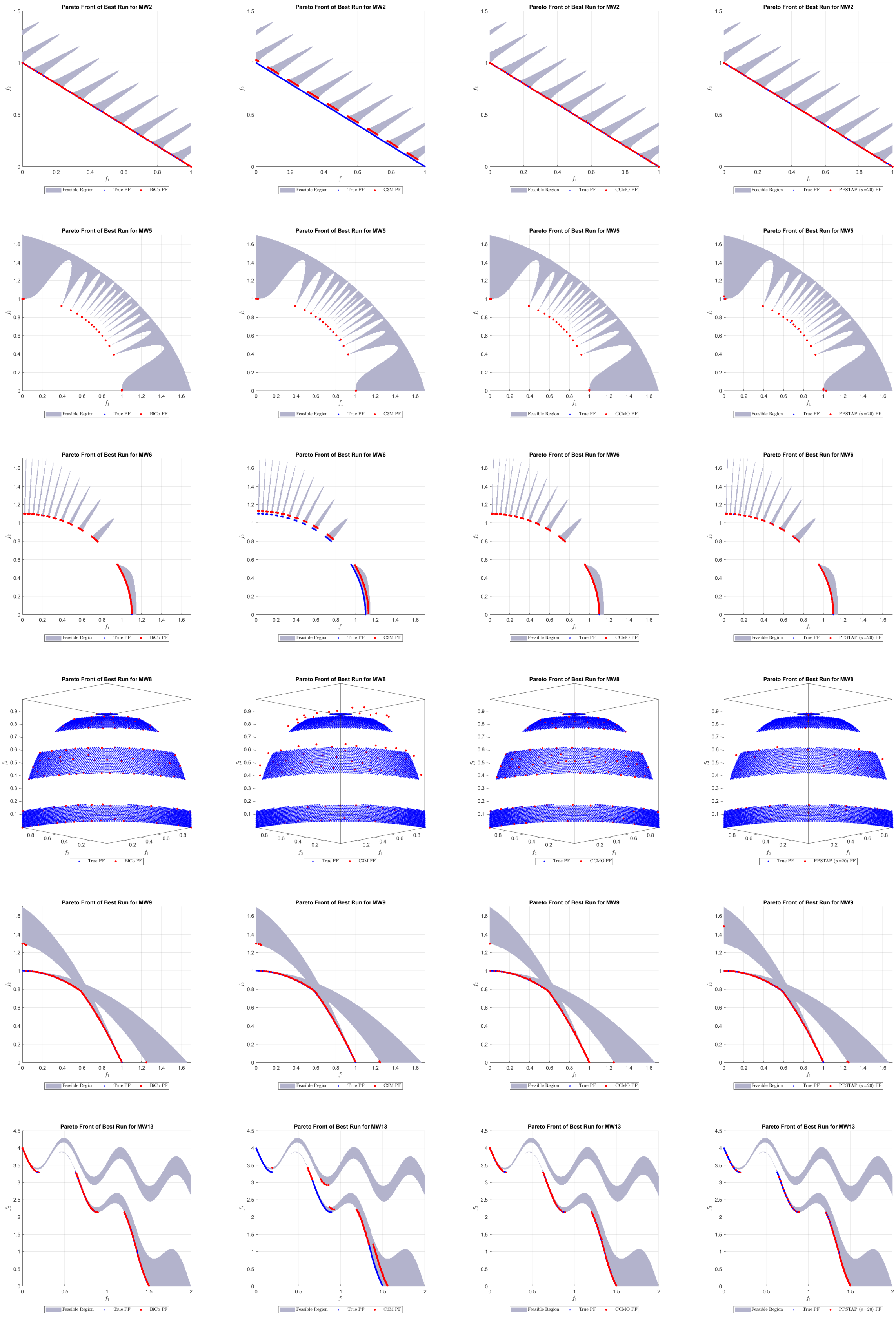

Figure 15. Best pareto fronts for selected MW problems in the sensitivity analysis.

Table 11. Wilcoxon test results for comparative analysis (Ref.: PPSTAP, p =20).

Meric	Competitor	CF	DASCMOP	LIRCMOP	MW	Overall
IGD	BiCo	1/8/1	5/4/0	0/14/0	9/4/1	15/30/2
	C3M	3/5/2	6/3/0	3/6/5	5/9/0	17/23/7
	CCMO	0/6/4	4/5/0	3/11/0	9/5/0	16/27/4
HV	BiCo	0/9/1	4/4/1	0/14/0	8/4/2	12/31/4
	C3M	4/6/0	6/2/1	6/7/1	4/9/1	20/24/3
	CCMO	1/7/2	4/5/0	3/11/0	9/5/0	17/28/2
IGDp	BiCo	1/8/1	5/4/0	0/14/0	9/4/1	15/30/2
	C3M	3/5/2	6/3/0	3/6/5	5/9/0	17/23/7
	CCMO	0/6/4	4/5/0	3/11/0	9/5/0	16/27/4

Table 12. Friedman test results for comparative analysis (Ref.: PPSTAP, p = 20).

Metric	Competitor	CF	DASCMOP	LIRCMOP	MW	Overall
IGD	BiCo	0/8/1	1/4/0	0/14/0	6/1/3	7/27/4
	C3M	3/3/3	4/0/1	3/5/6	3/5/2	13/13/12
	CCMO	0/6/3	1/4/0	3/11/0	7/2/1	11/23/4
HV	BiCo	0/8/1	0/4/1	0/14/0	5/1/4	5/27/6
	C3M	3/4/2	3/0/2	4/5/5	3/6/1	13/15/10
	CCMO	0/5/4	1/4/0	3/11/0	7/3/0	11/23/4
IGDp	BiCo	1/7/1	1/4/0	0/14/0	6/1/3	8/26/4
	C3M	3/3/3	4/0/1	2/5/7	3/5/2	12/13/13
	CCMO	0/4/5	1/4/0	3/11/0	6/3/1	10/22/6

6. Experimental results discussion

In this study, PPSTAP, we propose a hybrid framework that integrates PPS and CMOEA/D-TAP. PPSTAP introduces a sensitivity parameter, p, which determines the proportion of function evaluations allocated to the push phase before switching to the pull phase. To investigate its influence on search performance, a comprehensive sensitivity analysis of p is conducted. Subsequently, the best-performing configuration is evaluated against state-of-the-art algorithms through a comparative analysis. The simulation results are presented from these two perspectives, and the key findings are discussed in the following sections.

6.1. Sensitivity analysis

The effect of parameter p is examined from multiple perspectives in the following sections.

6.1.1. Best mean performance

The influence of the switching parameter p is first analyzed using the best mean values reported in Tables 1–3. All PPSTAP variants demonstrate improvements over CMOEA/D-TAP, confirming the effectiveness of the proposed framework. Although PPS achieves a slightly higher number of best mean values than PPSTAP (p =20) across the three indicators, PPSTAP (p =20) provides the most balanced and consistent performance across the benchmark suites. The remaining variants, PPSTAP (p =10), PPSTAP (p =30), and PPSTAP (p =40), achieve the best results for some individual problems; however, these gains are problem-dependent rather than consistent. Therefore, PPSTAP (p =20) is selected as the representative configuration.

6.1.2. Wilcoxon rank-sum test results

Tables 4–6 report the Wilcoxon rank-sum test results for IGD, HV, and IGDp. Compared with CMOEA/D-TAP, all PPSTAP variants achieve considerably more statistically significant wins than losses, with PPSTAP (p =20) showing the strongest overall advantage, followed by PPSTAP (p =10), PPSTAP (p =40), and PPSTAP (p =30). Against PPS, all variants remain competitive, with PPSTAP (p =20) obtaining the highest number of significant improvements, while the other settings maintain favorable win-to-loss ratios. The mutual comparison among PPSTAP variants indicates that no alternative value of p provides a consistent statistical advantage over PPSTAP (p =20), as most comparisons result in statistically equivalent outcomes.

6.1.3. Friedman test results

The Friedman test results in Table 7 further examine the relative rankings of the PPSTAP variants using PPSTAP (p =20) as the reference. All variants achieve better rankings than CMOEA/D-TAP across IGD, HV, and IGDp, reinforcing the effectiveness of the proposed approach. Compared with PPS, the variants remain competitive, although PPS obtains slightly better rankings for some suites, particularly LIRCMOP and MW. Among the proposed configurations, PPSTAP (p =20) achieves the most favorable overall ranking, whereas PPSTAP (p =10), PPSTAP (p =30), and PPSTAP (p =40) show improvements over CMOEA/D-TAP but lack consistent superiority over the selected setting. Therefore, PPSTAP (p =20) is adopted as the optimal configuration.

6.1.4. Convergence profiles of mean IGD, HV, and IGDp values

Figures 2–4 illustrate the convergence of the mean IGD, HV, and IGDp values for the first six problems of each benchmark suite. Overall, all PPSTAP variants improve solution quality throughout the search, although their convergence behavior differs with the parameter setting. PPSTAP (p =20) consistently converges faster, exhibits smoother search trajectories, and achieves superior final IGD, HV, and IGDp values on most problems. PPSTAP (p =30) remains competitive but generally converges more slowly and attains slightly inferior final performance, whereas PPSTAP (p =40) shows greater fluctuations and delayed convergence, particularly for challenging CMOPs. The temporary disappearance of some curves indicates the absence of feasible solutions at those stages, preventing the corresponding indicator from being computed until feasibility is restored. The observed fluctuations further reflect the difficulty of maintaining feasible solutions while balancing convergence and diversity. Nevertheless, all variants recover and continue improving, with PPSTAP (p =20) demonstrating the most stable convergence and overall best search performance.

6.1.5. Coverage of the approximated pareto fronts

The Pareto fronts for selected problems in the CF, DASCMOP, LIRCMOP, and MW suites, shown in Figures 5–8, reveal noticeable differences among PPS, CMOEA/D-TAP, and the PPSTAP variants. PPS separates exploration from constraint handling through push and pull stages. An untimely transition may limit either exploration or final feasible refinement. Its MOEA/D decomposition may also reduce coverage of disconnected or irregular fronts. CMOEA/D-TAP avoids an explicit stage transition but remains dependent on decomposition and threshold-adaptive penalty. Hard constraints can further restrict feasible search directions and slow population movement toward the CPF, causing delayed convergence and incomplete coverage. PPSTAP shares the decomposition limitation and is sensitive to p. A small p may restrict exploration, whereas a large p may leave insufficient budget for constrained refinement. Although $p=20\%$ provides the best average balance, it is not necessarily optimal for every problem. Thus, the observed variations mainly reflect decomposition-induced search bias, hard-constraint effects, and the exploration–refinement trade-off.

6.2. Comparative analysis

The performance of the best-performing variant, PPSTAP ($p=20$), is evaluated against state-of-the-art algorithms from multiple perspectives in the following sections. For brevity, PPSTAP hereafter refers to PPSTAP ($p=20$) unless otherwise stated.

6.2.1. Best mean performance

Tables 8–10 report the mean and standard deviation of the IGD, HV, and IGDp metrics. The proposed variant, PPSTAP ($p=20$), demonstrates highly competitive performance against the state-of-the-art algorithms across all benchmark suites. It achieves the highest number of best mean values on the LIRCMOP and MW suites for all indicators, reflecting its effectiveness in maintaining a desirable balance between convergence and diversity on challenging constrained multiobjective problems. Furthermore, PPSTAP attains superior results for several CF and DASCMOP instances. Although C3M remains competitive on several CF and DASCMOP problems and CCMO performs favourably on some DASCMOP and LIRCMOP cases, BiCo achieves limited best results. Overall, no single algorithm dominates all benchmark suites; however, PPSTAP exhibits the most extensive superiority on the challenging LIRCMOP and MW suites, demonstrating its robustness across constrained optimization scenarios.

6.2.2. Wilcoxon rank-sum test results

The Wilcoxon Rank-Sum test results in Table 11 provide a statistical comparison between PPSTAP ($p=20$) and the competing algorithms. PPSTAP achieves a favorable win-to-loss ratio on the CF and DASCMOP suites across IGD, HV, and IGDp, confirming its stable convergence and diversity performance under varying constraint conditions. The most notable advantage is observed for the LIRCMOP suite, where PPSTAP significantly outperforms BiCo and CCMO, achieving 14 and 11 wins for IGD and HV, respectively, without being outperformed on any problem. This highlights the effectiveness of the threshold adaptive penalty mechanism in addressing highly constrained problems. PPSTAP also maintains competitive superiority for the MW suite. Overall, PPSTAP achieves 30, 23, and 27 wins against BiCo, C3M, and CCMO for IGD, and 31, 24, and 28 wins for HV, respectively.

The consistent trend in IGDp further confirms the reliability of the proposed approach.

6.2.3. Friedman test

The Friedman test results in Table 12 further validate the ranking superiority of PPSTAP (p =20) over the competing algorithms. PPSTAP achieves favorable rankings on the CF and DASCMOP suites, indicating stable performance across constraint landscapes. The LIRCMOP suite again demonstrates the clear advantage of PPSTAP, where it surpasses BiCo on 14 problems for all indicators and maintains competitive rankings against CCMO. For the MW suite, PPSTAP preserves its competitive ranking performance, particularly compared with C3M. Overall, PPSTAP achieves the most favorable rankings among the compared algorithms, outperforming BiCo, C3M, and CCMO on 27, 13, and 23 problems for IGD, respectively, with consistent trends observed for HV and IGDp. These results further verify that the integration of push–pull search with threshold adaptive penalty handling provides an effective and robust solution for constrained multiobjective optimization.

6.2.4. Convergence profiles of mean IGD, HV, and IGDp values

Figures 9–11 illustrate the convergence of the mean IGD, HV, and IGDp values for the first six problems of each benchmark suite. Overall, PPSTAP (p =20) exhibits fast and stable convergence, reaching the best or highly competitive final performance on most problems. BiCo is generally the closest competitor, showing similar convergence trends on several instances but often ending with inferior IGD, IGDp, or HV values. C3M performs competitively on selected problems; however, its convergence is less consistent, with noticeable oscillations and occasional premature stagnation. In contrast, CCMO converges more slowly and encounters greater difficulty in obtaining high-quality feasible solutions, particularly on the challenging DASCMOP and LIRCMOP problems. The temporary disappearance of some convergence curves indicates stages where no feasible solutions are available, preventing the corresponding performance indicators from being evaluated. These fluctuations further highlight differences in the ability of the algorithms to maintain feasible and well-distributed solutions during the search. Although all algorithms continue to improve after feasible solutions are recovered, PPSTAP (p =20) generally follows a more stable search trajectory and achieves consistently competitive final performance across most benchmark problems.

6.2.5. Coverage of the approximated pareto fronts

Across the CF, DASCMOP, LIRCMOP, and MW suites, the final-front distributions displayed for selected problems in Figures 12–15 show clear differences among the four methods. BiCo divides the search between feasible and infeasible populations. Restricted mating may limit information transfer between them. This can cause local concentration and incomplete front coverage. C3M enables broad initial exploration through its feasibility-free stage. However, priority-based constraint handling can gradually narrow the search. Less informative constraint priorities may further reduce diversity. CCMO also uses two complementary populations. Their cooperation may become biased toward feasibility. This can reduce exploration of less-represented regions. PPSTAP (p =20) provides a more balanced search. It first explores the objective space and then performs constraint-focused refinement using threshold-adaptive penalty and MOEA/D decomposition. However, decomposition may be less effective for discontinuous or disconnected fronts. Moreover, p=20% is selected based on average performance across the tested instances. It is therefore not optimal for every problem. An unsuitable p may either restrict exploration or leave insufficient budget for final constrained refinement. These factors explain the observed differences in front coverage, solution concentration, and convergence quality across the tested suites.

7. Conclusions and future work

7.1. Conclusions

In this study, PPSTAP, a constrained multiobjective evolutionary algorithm that integrates a push–pull search strategy with an NFT-based adaptive penalty mechanism within the MOEA/D framework, is proposed. Extensive experiments on four benchmark suites demonstrated the effectiveness of the proposed approach. The sensitivity analysis showed that all PPSTAP variants outperformed their parent algorithms, PPS and CMOEA/D-TAP, on average according to the employed statistical tests. Among the proposed variants, PPSTAP (p =20) achieved the best overall performance and exhibited robust convergence, solution diversity, and stability. Comparative results further showed that PPSTAP (p =20) is competitive with state-of-the-art constrained multiobjective evolutionary algorithms across constraint landscapes. Overall, the proposed integration effectively balances exploration, exploitation, and constraint handling, making PPSTAP a robust and competitive approach for constrained multiobjective optimization.

7.2. Future work

In future work, this study can be extended in the following directions:

- To assess the effectiveness of PPSTAP on additional benchmark suites as well as real-world constrained multiobjective optimization problems.
- To investigate the integration of alternative penalty functions within the PPSTAP framework to enhance constraint-handling capability.
- To extend and adapt PPSTAP for solving dynamic constrained multiobjective optimization problems (DCMOPs).

Author contributions

Muhammad Sagheer: Conceptualization, Methodology, Investigation, Validation, Software, Formal Analysis, Writing original draft, Writing review and editing; Muhammad Asif Jan: Conceptualization, Methodology, Investigation, Software, Formal Analysis, Writing original draft, Supervision; Akhtar Munir Khan: Conceptualization, Methodology, Software, Writing original draft; Emel Khan: Investigation, Validation, Formal Analysis, Writing review and editing, Supervision; Farman Shah: Investigation, Validation, Writing review and editing. All authors have read and agreed to the published version of the manuscript.

Use of Generative-AI tools declaration

The authors declare that they have not used Artificial Intelligence (AI) tools in the creation of this article.

Conflict of interest

The authors state that they do not have any conflicts of interest.

References

1. K. Miettinen, *Nonlinear multiobjective optimization*, Berlin: Springer, 1999.
2. K. Deb, *Multi-Objective Optimisation Using Evolutionary Algorithms: An Introduction*, Berlin: Springer, 2011.
3. Q. Zhang, H. Li, MOEA/D: A multiobjective evolutionary algorithm based on decomposition, *IEEE Trans. Evol. Comput.*, **11** (2007), 712–731. https://doi.org/10.1109/TEVC.2007.892759
4. J. Liang, X. Ban, K. Yu, B. Qu, K. Qiao, C. Yue, et al., A survey on evolutionary constrained multiobjective optimization, *IEEE Trans. Evol. Comput.*, **27** (2023), 201–221. https://doi.org/10.1109/TEVC.2022.3155533
5. R. Saravanan, S. Ramabalan, N. G. R. Ebenezer, C. Dharmaraja, Evolutionary multi criteria design optimization of robot grippers, *Appl. Soft Comput.*, **9** (2009), 159–172. https://doi.org/10.1016/j.asoc.2008.04.001
6. M. Basu, Economic environmental dispatch using multi-objective differential evolution, *Appl. Soft Comput.*, **11** (2011), 2845–2853. https://doi.org/10.1016/j.asoc.2010.11.014
7. X. Zuo, C. Chen, W. Tan, M. Zhou, Vehicle scheduling of an urban bus line via an improved multiobjective genetic algorithm, *IEEE Trans. Intell. Transport. Syst.*, **16** (2014), 1030–1041. https://doi.org/10.1109/TITS.2014.2352599
8. Y. Cui, Z. Geng, Q. Zhu, Y. Han, Multi-objective optimization methods and application in energy saving, *Energy*, **125** (2017), 681–704. https://doi.org/10.1016/j.energy.2017.02.174
9. M. Premkumar, P. Jangir, B. S. Kumar, R. Sowmya, H. H. Alhelou, L. Abualigah, et al., A new arithmetic optimization algorithm for solving real-world multiobjective cec-2021 constrained optimization problems: Diversity analysis and validations, *IEEE Access*, **9** (2021), 84263–84295. https://doi.org/10.1109/ACCESS.2021.3085529
10. M. Niu, C. Wan, Z. Xu, A review on applications of heuristic optimization algorithms for optimal power flow in modern power systems, *J. Modern Power Syst. Clean Energy*, **2** (2014), 289–297. https://doi.org/10.1007/s40565-014-0089-4
11. N. Srinivas, K. Deb, Muiltiobjective optimization using nondominated sorting in genetic algorithms, *Evol. Comput.*, **2** (1994), 221–248. https://doi.org/10.1162/evco.1994.2.3.221
12. K. Deb, A. Pratap, S. Agarwal, T. Meyarivan, A fast and elitist multiobjective genetic algorithm: NSGA-II, *IEEE Trans. Evol. Comput.*, **6** (2002), 182–197. https://doi.org/10.1109/4235.996017

13. K. Deb, H. Jain, An evolutionary many-objective optimization algorithm using reference-point-based nondominated sorting approach, part I: Solving problems with box constraints, *IEEE Trans. Evol. Comput.*, **18** (2014), 577–601. https://doi.org/10.1109/TEVC.2013.2281535

14. T. Murata, H. Ishibuchi, MOGA: Multi-objective genetic algorithms, *IEEE Int. Confer. Evol. Comput.*, **1** (1995), 289–294. https://doi.org/10.1109/ICEC.1995.489161

15. J. Horn, N. Nafpliotis, D. E. Goldberg, A niched Pareto genetic algorithm for multiobjective optimization, In: *Proceedings of the First IEEE Conference on Evolutionary Computation. IEEE World Congress on Computational Intelligence*, Orlando: IEEE, 1994, 82–87. https://doi.org/10.1109/ICEC.1994.350037

16. E. Zitzler, L. Thiele, Multiobjective evolutionary algorithms: A comparative case study and the strength Pareto approach, *IEEE Trans. Evol. Comput.*, **3** (1999), 257–271. https://doi.org/10.1109/4235.797969

17. E. Zitzler, M. Laumanns, L. Thiele, SPEA2: Improving the strength Pareto evolutionary algorithm, *TIK Report*, 2001. https://doi.org/10.3929/ethz-a-004284029

18. D. W. Corne, J. D. Knowles, M. J. Oates, The Pareto envelope-based selection algorithm for multiobjective optimization, In: *International Conference on Parallel Problem Solving from Nature*, Berlin: Springer, 2000, 839–848. https://doi.org/10.1007/3-540-45356-3_82

19. Y. Chen, W. H. Chan, E. L. M. Su, Q. Diao, Multi-objective optimization for smart cities: A systematic review of algorithms, challenges, and future directions, *Peer J Comput. Sci.*, **11** (2025), e3042. https://doi.org/10.7717/peerj-cs.3042

20. M. G. de Alcantara, A. F. da Silva, F. A. S. Marins, R. de Carvalho Miranda, Systematic literature review on multi-objective simulation optimization, *Complex Syst. Model. Simul.*, **5** (2025), 190–220. https://doi.org/10.23919/CSMS.2024.0037

21. E. Zitzler, S. Künzli, Indicator-based selection in multiobjective search, In: *International Conference on Parallel Problem Solving from Nature*, Berlin: Springer, 2004, 832–842. https://doi.org/10.1007/978-3-540-30217-9_84

22. J. Bader, E. Zitzler, Hype: An algorithm for fast hypervolume-based many-objective optimization, *Evol. Comput.*, **19** (2011), 45–76. https://doi.org/10.1162/EVCO_a_00009

23. D. H. Phan, J. Suzuki, R2-IBEA: R2 indicator based evolutionary algorithm for multiobjective optimization, In: *2013 IEEE Congress on Evolutionary Computation*, Cancun: IEEE, 2013. https://doi.org/10.1109/CEC.2013.6557783

24. T. Zheng, J. Liu, S. Tan, H. Wang, An indicator based multiobjective evolutionary algorithm utilizing inverse modeling, In: *2024 43rd Chinese Control Conference (CCC)*, Kunming: IEEE, 2024, 2088–2093. https://doi.org/10.23919/CCC63176.2024.10661744

25. H. Li, Q. Zhang, Multiobjective optimization problems with complicated Pareto sets, MOEA/D and NSGA-II, *IEEE Trans. Evol. Comput.*, **13** (2008), 284–302. https://doi.org/10.1109/TEVC.2008.925798

26. Q. Zhang, W. Liu, H. Li, The performance of a new version of MOEA/D on CEC09 unconstrained MOP test instances, In: *2009 IEEE Congress on Evolutionary Computation*, Trondheim: IEEE, 2009, 203–208. https://doi.org/10.1109/CEC.2009.4982949

27. K. Li, K. Deb, Q. Zhang, S. Kwong, An evolutionary many-objective optimization algorithm based on dominance and decomposition, *IEEE Trans. Evol. Comput.*, **19** (2014), 694–716. https://doi.org/10.1109/TEVC.2014.2373386
28. Y. Qi, X. Ma, F. Liu, L. Jiao, J. Sun, J. Wu, MOEA/D with adaptive weight adjustment, *Evol. Comput.*, **22** (2014), 231–264. https://doi.org/10.1162/EVCO_a_00109
29. L. R. de Farias, A. F. Araújo, A decomposition-based many-objective evolutionary algorithm updating weights when required, *Swarm Evol. Comput.*, **68** (2022), 100980. https://doi.org/10.1016/j.swevo.2021.100980
30. J. Qiao, H. Zhou, C. Yang, S. Yang, A decomposition-based multiobjective evolutionary algorithm with angle-based adaptive penalty, *Appl. Soft Comput.*, **74** (2019), 190–205. https://doi.org/10.1016/j.asoc.2018.10.028
31. Y. Zhu, Y. Qin, D. Yang, H. Xu, H. Zhou, An enhanced decomposition-based multi-objective evolutionary algorithm with a self-organizing collaborative scheme, *Expert Syst. Appl.*, **213** (2023), 118915. https://doi.org/10.1016/j.eswa.2022.118915
32. H. Cheng, L. Li, L. You, A weight vector adjustment method for decomposition-based multi-objective evolutionary algorithms, *IEEE Access*, **11** (2023), 42324–42330. https://doi.org/10.1109/ACCESS.2023.3270806
33. Y. Su, Q. Lin, Z. Ming, K. C. Tan, Adapting decomposed directions for evolutionary multiobjective optimization, *IEEE Trans. Cyber.*, **53** (2022), 6289–6302. https://doi.org/10.1109/TCYB.2022.3165557
34. J. Wang, Y. Su, Q. Lin, L. Ma, D. Gong, J. Li, et al., A survey of decomposition approaches in multiobjective evolutionary algorithms, *Neurocomputing*, **408** (2020), 308–330. https://doi.org/10.1016/j.neucom.2020.01.114
35. Y. Su, J. Wang, L. Ma, X. Wang, Q. Lin, C. A. C. Coello, et al., A hybridized angle-encouragement-based decomposition approach for many-objective optimization problems, *Appl. Soft Comput.*, **78** (2019), 355–372. https://doi.org/10.1016/j.asoc.2019.02.026
36. Y. Su, Q. Lin, J. Wang, J. Li, J. Chen, Z. Ming, A constrained solution update strategy for multiobjective evolutionary algorithm based on decomposition, *Complexity*, **2019** (2019), 3251349. https://doi.org/10.1155/2019/3251349
37. E. Mezura-Montes, C. A. C. Coello, Constraint-handling in nature-inspired numerical optimization: Past, present and future, *Swarm Evol. Comput.*, **1** (2011), 173–194. https://doi.org/10.1016/j.swevo.2011.10.001
38. T. Runarsson, X. Yao, Evolutionary search and constraint violations, In: *The 2003 Congress on Evolutionary Computation*, Canberra: IEEE, 2003. https://doi.org/10.1109/CEC.2003.1299836
39. M. A. Jan, M. Sagheer, H. U. Khan, M. I. Uddin, R. A. Khanum, M. Mahmoud, et al., Hybrid stochastic ranking for constrained optimization, *IEEE Access*, **8** (2020), 227270–227287. https://doi.org/10.1109/ACCESS.2020.3044439
40. C. Wang, R. Xu, An angle based evolutionary algorithm with infeasibility information for constrained many-objective optimization, *Appl. Soft Comput.*, **86** (2020), 105911. https://doi.org/10.1016/j.asoc.2019.105911

41. Y. Hao, C. Zhao, Y. Zhang, Y. Cao, Z. Li, Constrained multi-objective optimization problems: Methodologies, algorithms and applications, *Knowledge-Based Syst.*, **299** (2024), 111998. https://doi.org/10.1016/j.knosys.2024.111998

42. R. Courant, Variational methods for the solution of problems of equilibrium and vibrations, *Bull. Amer. Math. Soc.*, **49** (1943), 1–23. https://doi.org/10.1090/S0002-9904-1943-07818-4

43. C. W. Carroll, The created response surface technique for optimizing nonlinear, restrained systems, *Oper. Res.*, **9** (1961), 169–184. https://doi.org/10.1287/opre.9.2.169

44. A. V. Fiacco, G. P. McCormick, Extensions of sumt for nonlinear programming: Equality constraints and extrapolation, *Manag. Sci.*, **12** (1966), 816–828. https://doi.org/10.1287/mnsc.12.11.816

45. M. A. Jan, Q. Zhang, MOEA/D for constrained multiobjective optimization: Some preliminary experimental results, In: *2010 UK Workshop on Computational Intelligence (UKCI)*, Colchester: IEEE, 2010. https://doi.org/10.1109/UKCI.2010.5625585

46. M. A. Jan, R. A. Khanum, N. M. Tairan, W. K. Mashwani, Performance of a constrained version of MOEA/D on CTP-series test instances, *Int. J. Adv. Comput. Sci. Appl.*, **7** (2016), 196–505.

47. H. Jain, K. Deb, An evolutionary many-objective optimization algorithm using reference-point based nondominated sorting approach, part ii: Handling constraints and extending to an adaptive approach, *IEEE Trans. Evol. Comput.*, **18** (2014), 602–622. https://doi.org/10.1109/TEVC.2013.2281534

48. K. Deb, An efficient constraint handling method for genetic algorithms, *Comput. Meth. Appl. Mech. Eng.*, **186** (2000), 311–338. https://doi.org/10.1016/S0045-7825(99)00389-8

49. Z. Z. Liu, B. C. Wang, K. Tang, Handling constrained multiobjective optimization problems via bidirectional coevolution, *IEEE Trans. Cyber.*, **52** (2022), 10163–10176. https://doi.org/10.1109/TCYB.2021.3056176

50. J. Zhou, J. Zou, S. Yang, J. Zheng, D. Gong, T. Pei, Niche-based and angle-based selection strategies for many-objective evolutionary optimization, *Inform. Sci.*, **571** (2021), 133–153. https://doi.org/10.1016/j.ins.2021.04.050

51. M. Asafuddoula, T. Ray, R. Sarker, K. Alam, An adaptive constraint handling approach embedded MOEA/D, In: *2012 IEEE Congress on Evolutionary Computation*, Brisbane: IEEE, 2012. https://doi.org/10.1109/CEC.2012.6252868

52. J. Zou, R. Sun, S. Yang, J. Zheng, A dual-population algorithm based on alternative evolution and degeneration for solving constrained multi-objective optimization problems, *Inform. Sci.*, **579** (2021), 89–102. https://doi.org/10.1016/j.ins.2021.07.078

53. Y. Tian, T. Zhang, J. Xiao, X. Zhang, Y. Jin, A coevolutionary framework for constrained multiobjective optimization problems, *IEEE Trans. Evol. Comput.*, **25** (2020), 102–116. https://doi.org/10.1109/TEVC.2020.3004012

54. Y. Tian, Y. Zhang, Y. Su, X. Zhang, K. C. Tan, Y. Jin, Balancing objective optimization and constraint satisfaction in constrained evolutionary multiobjective optimization, *IEEE Trans. Cyber.*, **52** (2022), 9559–9572. https://doi.org/10.1109/TCYB.2020.3021138

55. Z. Z. Liu, Y. Wang, Handling constrained multiobjective optimization problems with constraints in both the decision and objective spaces, *IEEE Trans. Evol. Comput.*, **23** (2019), 870–884. https://doi.org/10.1109/TEVC.2019.2894743

56. R. Sun, J. Zou, Y. Liu, S. Yang, J. Zheng, A multistage algorithm for solving multiobjective optimization problems with multiconstraints, *IEEE Trans. Evol. Comput.*, **27** (2023), 1207–1219. https://doi.org/10.1109/TEVC.2022.3224600

57. Z. Fan, W. Li, X. Cai, H. Li, C. Wei, Q. Zhang, et al., Push and pull search for solving constrained multi-objective optimization problems, *Swarm Evol. Comput.*, **44** (2019), 665–679. https://doi.org/10.1016/j.swevo.2018.08.017

58. A. M. Khan, M. A. Jan, M. Sagheer, R. A. Khanum, M. I. Uddin, S. Ahmad, Near feasibility driven adaptive penalty functions embedded MOEA/D, *IEEE Access*, **11** (2023), 105182–105213. https://doi.org/10.1109/ACCESS.2023.3317818

59. Y. Tian, R. Cheng, X. Zhang, Y. Jin, PlatEMO: A MATLAB platform for evolutionary multi-objective optimization [educational forum], *IEEE Comput. Intell. Magaz.*, **12** (2017), 73–87. https://doi.org/10.1109/MCI.2017.2742868

60. Q. Zhang, A. Zhou, S. Zhao, P. N. Suganthan, W. Liu, S. Tiwari, Multiobjective optimization test instances for the cec 2009 special session and competition, Technical report, In: *University of Essex, Colchester, UK and Nanyang Technological University, Singapore, Special Session on Performance Assessment of Multi-Objective Optimization Algorithms*, **264** (2008), 1–30.

61. Z. Fan, W. Li, X. Cai, H. Huang, Y. Fang, Y. You, et al., An improved epsilon constraint-handling method in MOEA/D for CMOPs with large infeasible regions, *Soft Comput.*, **23** (2019), 12491–12510. https://doi.org/10.1007/s00500-019-03794-x

62. Z. Fan, W. Li, X. Cai, H. Li, C. Wei, Q. Zhang, et al., Difficulty adjustable and scalable constrained multiobjective test problem toolkit, *Evol. Comput.*, **28** (2020), 339–378. https://doi.org/10.1162/evco_a_00259

63. Z. Ma, Y. Wang, Evolutionary constrained multiobjective optimization: Test suite construction and performance comparisons, *IEEE Trans. Evol. Comput.*, **23** (2019), 972–986. https://doi.org/10.1109/TEVC.2019.2896967

64. A. Mohammadi, M. N. Omidvar, X. Li, A new performance metric for user-preference based multi-objective evolutionary algorithms, In: *2013 IEEE Congress on Evolutionary Computation*, Cancun: IEEE, 2013, 2825–2832. https://doi.org/10.1109/CEC.2013.6557912

65. C. A. C. Coello, N. C. Cortés, Solving multiobjective optimization problems using an artificial immune system, *Genet. Program Evolvable Mach.*, **6** (2005), 163–190. https://doi.org/10.1007/s10710-005-6164-x

66. D. A. Van Veldhuizen, *Multiobjective Evolutionary Algorithms: Classifications, Analyses, and New Innovations*, Dayton: Air Force Institute of Technology, 1999.

67. E. Zitzler, L. Thiele, Multiobjective optimization using evolutionary algorithms–a comparative case study, In: *International Conference on Parallel Problem Solving from Nature*, Berlin: Springer, 1998, 292–301. https://doi.org/10.1007/BFb0056872

68. H. Ishibuchi, H. Masuda, Y. Tanigaki, Y. Nojima, Modified distance calculation in generational distance and inverted generational distance, In: *International Conference on Evolutionary Multi-Criterion Optimization*, 2015, 110–125. https://doi.org/10.1007/978-3-319-15892-1_8

69. H. Ishibuchi, R. Imada, N. Masuyama, Y. Nojima, Comparison of hypervolume, IGD and IGD+ from the viewpoint of optimal distributions of solutions, In: *International Conference on Evolutionary Multi-Criterion Optimization*, 2019, 332–345. https://doi.org/10.1007/978-3-030-12598-1_27

70. E. Zitzler, J. Knowles, L. Thiele, Quality assessment of pareto set approximations, In: *Multiobjective Optimization: Interactive and Evolutionary Approaches*, Berlin: Springer, 2008, 373–404. https://doi.org/10.1007/978-3-540-88908-3_14

AIMS Press

© 2026 the Author(s), licensee AIMS Press. This is an open access article distributed under the terms of the Creative Commons Attribution License (https://creativecommons.org/licenses/by/4.0)